UNIVERSIDAD DE INVESTIGACIÓN DE TECNOLOGÍA EXPERIMENTAL YACHAY

Escuela de Ciencias Físicas y Nanotecnología

TÍTULO: Collective Behaviors Induced by Heterogeneity in Dynamical Networks

Trabajo de integración curricular presentado como requisito para la obtención del título de Físico

Autor:
Robalino Gómez Kevin Alexis

Tutor:
PhD. Cosenza Miceli Mario Giuseppe

Urcuquí - Octubre 2023

Autoría

Yo, **Robalino Gómez Kevin Alexis**, con cedula de identidad **0605698562**, declaro que las ideas, juicios, valoraciones, interpretaciones, consultas bibliográficas, definiciones y conceptualizaciones expuestas en el presente trabajo; así cómo, los procedimientos y herramientas utilizadas en la investigación, son de absoluta responsabilidad de el autor del trabajo de integracion curricular. Así mismo, me acojo a los reglamentos internos de la Universidad de Investigación de Tecnología Experimental Yachay.

Urcuquí, Octubre 2023

Firmado electrónicamente por:
KEVIN ALEXIS
ROBALINO GOMEZ

Kevin Alexis Robalino Gómez
CI: 0605698562

Autorizacion de publicación

Yo, **Robalino Gómez Kevin Alexis**, con cedula de identidad **0605698562**, cedo a la Universidad de Investigación de Tecnología Experimental Yachay, los derechos de publicación de la presente obra, sin que deba haber un reconocimiento económico por este concepto. Declaro además que el texto del presente trabajo de titulación no podrá ser cedido a ninguna empresa editorial para su publicación u otros fines, sin contar previamente con la autorización escrita de la Universidad.
Asimismo, autorizo a la Universidad que realice la digitalización y publicación de este trabajo de integración curricular en el repositorio virtual, de conformidad a lo dispuesto en el Art. 144 de la Ley Orgánica de Educación Superior.

Urcuquí, Octubre 2023

Firmado electrónicamente por:
KEVIN ALEXIS
ROBALINO GOMEZ

Kevin Alexis Robalino Gómez
CI: 0605698562

Dedication

I dedicate this work to my parents: Alicia and Rene who have been my inspiration and unconditional support. This work is only the fruit of your efforts. I dedicate it to my brothers, my uncles, and cousins who have never hesitated to give me their help and love.

Kevin Alexis Robalino Gómez

Acknowledgements

This work would not be possible without the help, inspiration, mentoring and friendship of my Advisor Mario Cosenza whom I admire, respect and appreciate, I deeply hope to become a wonderful professional and person like him. Thanks to Yachay Tech University for this great opportunity to meet all the professors who have guided my education.

The culmination of my higher education would not have been possible without the support and love of my parents during all these years. All the effort, dedication, and work required to complete my studies was possible thanks to the support and help of the people I met at the university who ended up becoming very dear friends. A special thanks to all my friends who supported me during this time. Last but not least I want to thank me for all the time and dedication.

Kevin Alexis Robalino Gómez

Resumen

Recientemente se ha descubierto un fenómeno denominado simetría inducida por asimetría en redes de elementos dinámicos que interactúan. Aparece cuando el estado colectivo del sistema puede ser simétrico sólo cuando los elementos del sistema no lo son; la simetría se refiere principalmente a un estado de sincronización. Esta situación puede interpretarse como la inversa del fenómeno conocido de ruptura de simetría, en el que el estado colectivo tiene menos simetría que los elementos. En esta Tesis, ampliamos la investigación de los procesos inducidos por asimetría a la aparición de otras formas de comportamientos colectivos en redes dinámicas, además de la sincronización. En particular, estudiamos el fenómeno del comportamiento colectivo no trivial -donde la periodicidad colectiva surge del caos local- inducido por la heterogeneidad en los parámetros locales. Investigamos un sistema de mapas globalmente acoplados como modelo de una red dinámica. Se emplean varios mapas locales que poseen caos robusto en un intervalo de sus parámetros. Definimos un parámetro de asimetría para caracterizar el grado de heterogeneidad del sistema. Comprobamos que la heterogeneidad de los parámetros de los elementos locales puede inducir una serie de comportamientos colectivos ordenados, periódicos y no triviales, distintos de la sincronización, en situaciones donde tales comportamientos no existen si el sistema es homogéneo. Nuestra investigación es relevante en muchos sistemas, como los sistemas sociales y biológicos, donde la diversidad y la heterogeneidad de los elementos ocurren comúnmente.
Palabras clave: Sistemas complejos, redes de mapas acoplados, comportamiento colectivo no trivial, simetría inducida por asimetría, sistemas heterogéneos.

Abstract

Recently, a phenomenon called asymmetry-induced symmetry has been discovered in networks of interacting dynamical elements. It appears when the collective state of the system can be symmetric only when the elements of system are not; symmetry mainly referring to a state of synchronization. This situation can be interpreted as the converse of the well known phenomenon of symmetry breaking, where the collective state has less symmetry than the elements. In this Thesis, we extend the investigation of asymmetry-induced processes to the emergence of other forms of collective behaviors in dynamical networks, besides synchronization. In particular, we study the phenomenon of nontrivial collective behavior –where collective periodicity arises from local chaos– induced by heterogeneity in the local parameters. We investigate a system of globally coupled maps as a model for a dynamical network. Several local maps possessing robust chaos on an interval of their parameters are employed. We define an asymmetry parameter to characterize the amount of heterogeneity in the system. We find that heterogeneity in the parameters of the local elements can induce a variety of ordered, periodic nontrivial collective behaviors, other than synchronization, in situations where such behaviors do not exist if the system is homogeneous. Our research is relevant in many systems, such as social and biological systems, where diversity and heterogeneity of the elements commonly occur.
Keywords: Complex systems, Coupled map networks, Nontrivial collective behavior, asymmetry-induced symmetry, heterogeneous systems.

Contents

1 Introduction **1**
1.1 Research problem . . . 2
1.2 Objectives . . . 2
1.2.1 General objective . . . 2
1.2.2 Specific objectives . . . 2

2 Theoretical framework: Synchronization induced by asymmetry **5**

3 Nontrivial collective behaviour in globally coupled map networks **9**

4 Heterogeneous dynamical networks: Results **13**
4.1 Heterogeneity/Asymmetry parameter . . . 13
4.2 Non-trivial collective behaviour induced by heterogeneity . . . 14
4.2.1 Heterogeneous network of logarithmic maps . . . 14
4.2.2 Heterogeneous network of singular maps . . . 18
4.2.3 Heterogeneous network of pincers maps: bounded robust chaos . . . 25
4.2.4 Heterogeneous network of smooth maps with robust chaos . . . 30

5 Conclusions **33**

Bibliography **35**

Appendices **38**

A Python code for Asymmetry parameter **41**

List of Figures

2.1 7-node network. The numbers in red and blue are the values of b_i, taken in the simulation, for the cases of homogeneous and heterogeneous distribution in that parameter, respectively. 6

2.2 Trajectories of the oscillators ($n = 7$). (a) Angular variable θ_i (relative to its average $\langle\theta_i\rangle$) vs t. (b) Amplitud variable r_i vs t. There is a desynchronized state with homogeneous values of $b_i = b^*$ for $t < 75$, followed by spontaneous synchronization with heterogeneity in b_i when $t \geq 75$. 6

2.3 Chaos synchronization induced by random oscillator heterogeneity. (a) Double-scroll chaotic attractor constructed from the experimental time series of the voltages V_x and V_y of a single uncoupled oscillator, and the time series for V_x shown separately. (b),(c) Corresponding experimental time series for oscillators in a directed ring for $k = 8.18$ (k controls the coupling strength). (b) and in a random network for $k = 5$. (c). Left: network structures and synchronization errors Z, where each node is labeled with its timescale τ_i. Right: time series after the initial transient (colored by oscillator) for initial conditions close to the synchronous state, showing that chaos synchronization is stable in the heterogeneous system but not in the homogeneous one. In particular, the heterogeneous systems both achieve low synchronization error and preserve qualitative properties of the original chaotic attractor. 7

3.1 Schematic representation of a globally coupled map network described by Eqs. (3.1). 10

3.2 Bifurcation diagram of the logarithmic map Eq. (3.2) as a function of the parameter b. Robust chaos occur for $b \in [-1, 1]$. x_1^* for $b < -1$ and x_2^* for $b > 1$ are fixed points. For each value of b, 100 iterates are shown, after discarding 1000 transient points. 10

3.3 Top: Time-evolution of the mean field h_t, Eq. (3.3), for the globally coupled system Eqs. (3.1), showing period two motion. Bottom: Time-evolution of the local map x^{1969} in the system Eqs. (3.1 exhibiting chaotic dynamics. Random initial conditions on the maps, uniformly distributed on the interval $x_0^i \in [-8, 4]$ are used for the globally coupled system Eqs. (3.1). Parameters for the system Eqs. (3.1) are $b = -0.7$, $\epsilon = 0.2$, $N = 10^5$. 11

3.4 Bifurcation diagram of the mean field h_t, Eq. (3.3), for the globally coupled system Eq. (3.1) as a function of the parameter b with fixed coupling $\epsilon = 0.25$. Size of the system $N = 10^5$. For each value of b, h_t is calculated for 100 time steps during a run starting from random initial conditions on the maps, uniformly distributed on the interval $x_0^i \in [-8, 4]$, after discarding 1000 transients. 11

3.5 Bifurcation diagram of the mean field h_t, Eq. (3.3), for the globally coupled system Eqs. (3.1) as a function of the coupling parameter ϵ, with a fixed value of the parameter $b = -0.7$ for the local maps. Size of the system $N = 10^5$. Random initial conditions are used for each value of ϵ, as in Fig. (3.4). 12

4.1 a) Bifurcation diagram logarithmic map Eq. (4.7) showing robust chaos in $b \in [-1, 1]$. For each value of b, 200 iterations are plotted after discarding 10^4 transients. b) Time series for 50 iterations, after discarding 10^4 iterations, for the logarithmic map with $b = 0.5$. 15
4.2 Globally coupled Logarithm maps. a) Bifurcation diagram for the mean field of the homogeneous network h_t as a function of the coupling parameter ϵ. b) Time average standard deviation $\langle\sigma\rangle$ vs. ϵ. In both graphs, initial conditions are uniformly distributed on the interval $x_0^i = [-8, 4]$, system size $N = 10^5$, and local parameters were fixed at $b = -0.7$. For each value of ϵ, 10^2 iterates are shown after discarding 10^3 transients. The vertical blue line signals the value $\epsilon = 0.85$. 15
4.3 a) Bifurcation diagram for the mean field of the network h_t vs. the asymmetry parameter A. b) Mean standard deviation $\langle\sigma\rangle$ as a function of the asymmetry parameter A. Fixed parameters are $\epsilon = 0.85$, size $N = 10^5$. For each value of A, 10^2 iterates are shown after discarding 10^3 transients. Initial conditions $x_0^i \in [-8, 4]$. 16
4.4 a) Bifurcation diagram h_t vs ϵ for the mean field of the maximum heterogeneous logarithmic map network, Eq. (4.9). b) $\langle\sigma\rangle$ vs ϵ. In both graphs, initial conditions are uniformly distributed on the interval $x_0^i = [-8, 4]$, system size $N = 10^5$, and local parameters are uniformly distributed at random $b_i \in [-1, 1]$ corresponding to $A = 1$. For each value of ϵ, 10^2 iterates are shown after discarding 10^3 transients. The vertical blue line signals the value $\epsilon = 0.85$. 17
4.5 Time series of the mean field h_t shows period three for the value $\epsilon = 0.85$ marked in Fig. (4.4). 50 iterations are shown after discarding 10^4 steps. 17
4.6 a) Bifurcation diagram of a singular map with $z = -0.25$ as a function of the parameter μ. For each value of μ, 100 iterations are shown after discarding 10^4 iterates . b) Chaotic time series of x_t for $z = -0.25$ and fixed $\mu = 1.1$ after discarding 10^4 iterates. 18
4.7 Critical boundaries $\mu_-(z)$ and $\mu_+(z)$ of the robust chaos region for the singular maps on the space of parameters (μ, z). 19
4.8 Globally coupled homogeneous singular maps Eqs. [4.12] with $z = -0.25$ and $\mu_i = 1.1$. a) Bifurcation diagram h_t vs ϵ. b) Mean standard deviation $\langle\sigma\rangle$ vs ϵ. In both graphs, initial conditions are uniformly distributed on the interval $x_0^i = [-8, 2]$, system size $N = 10^5$. For each value of ϵ, 10^2 iterates are shown after discarding 10^3 transients. The vertical blue line signals the value $\epsilon = 0.82$. 19
4.9 a) Time evolution of the mean field h_t for the homogeneous system Eqs. [4.12] with $z = -0.25$ and $\mu = 1.1$ and the coupling value $\epsilon = 0.1$ displaying period-two collective behaviour. b) Time evolution of one map in the network displaying chaotic dynamics coexisting with the collective periodic behavior. 20
4.10 a) Bifurcation diagram for the mean field h_t as a function of the asymmetry parameter A for the network of coupled singular maps Eqs. (4.12) with fixed coupling $\epsilon = 0.82$ and local maps with $z = -0.25$. b) Mean standard deviation $\langle\sigma\rangle$ vs. A. In both graphs, initial conditions are uniformly distributed on the interval $x_0^i = [-8, 2]$, system size $N = 10^5$. For each value of A, 10^2 iterates are shown after discarding 10^3 transients. 20
4.11 a) Bifurcation diagram for the mean field h_t as a function of the asymmetry parameter A for the network of coupled singular maps Eqs. (4.12) with fixed coupling $\epsilon = 0.82$ and local maps with $z = -0.25$. System size $N = 10^5$. b) Period-five collective behavior of h_t when $A = 0.609$, calculated over 20 iterations after discarding 10^4 transients. 21
4.12 a) Bifurcation diagram for the mean field h_t as a function of the asymmetry parameter A for the network of coupled singular maps Eqs. (4.12) with fixed coupling $\epsilon = 0.89$ and local maps with $z = -0.25$. The blue line signals the value $A = 0.809$. System size $N = 10^5$. b) Time series period-three collective behavior of h_t for the asymmetry parameter $A = 0.809$, calculated over 20 iterations after discarding 10^4 transients. . . 22

4.13 Globally coupled singular maps Eqs. [4.12] with $z = -0.25$ and maximum heterogeneity $A = 1$, corresponding to the local parameters distributed in the robust chaos range $\mu_i \in [0.98, 1.64]$. a) Bifurcation diagram h_t vs ϵ. b) Mean standard deviation $\langle\sigma\rangle$ vs ϵ. In both graphs, initial conditions are uniformly distributed on the interval $x_0^i = [-8, 2]$, system size $N = 10^5$. For each value of ϵ, 10^2 iterates are shown after discarding 10^3 transients. The vertical blue line signals the value $\epsilon = 0.82$. 22
4.14 a) Bifurcation diagram of a singular map with $z = 0.5$ as a function of μ. For each value of μ, 100 iterates are shown, after discarding 10^5 transients iterations. b) Time series of x_t for the parameter value $\mu = 0.5$, calculated over 50 iterations after discarding 10^4 transients. 23
4.15 Network of globally coupled singular maps Eqs. (4.12) with $z = 0.5$. a)-b) Homogeneous parameters $\mu_i = 0.5, \forall i$; bifurcation diagram for the mean field h_t vs. ϵ and $\langle\sigma\rangle$ vs. ϵ. c)-d) Maximum heterogeneity $\mu_i \in [0.25, 0.75]$; bifurcation diagram for the mean field h_t vs. ϵ and $\langle\sigma\rangle$ vs. ϵ. The blue line signals the value $\epsilon = 0.788$. e)-f) Fixed coupling $\epsilon = 0.788$; bifurcation diagram for the mean field h_t vs. A and $\langle\sigma\rangle$ vs. A. In all graphs, initial conditions are uniformly distributed on the interval $x_0^i = [-8, 2]$, system size $N = 10^5$. For each value of ϵ and A, 10^2 iterates are shown, after discarding 10^3 transients. 24
4.16 a) Bifurcation diagram for the pincer map Eq. (4.16) as a function of c, with fixed value $s = 1.3$, calculated over 200 iterations for each value of c, after discarding 10^4 iterations. b) Time series for $s = 1.3$, $c = 0.25$. 25
4.17 Globally coupled homogeneous pincers maps with $s = 1.3, c_i = 0.1$. a) h_t vs. ϵ. For each value of ϵ, 10^2 iterates are shown after 10^3 transients. b) $\langle\sigma\rangle$ vs. ϵ. Initial conditions are uniformly distributed $x_0^i \in [-0.3, 0.78]$, $N = 10^5$. 25
4.18 Globally coupled heterogeneous pincers maps with $s = 1.3, \epsilon = 0.47$ (blue line in Fig, (4.17)a), and asymmetry parameter A according to Eq. (4.17). a) Bifurcation diagram of h_t vs. A, . b) $\langle\sigma\rangle$ vs. A. Initial conditions are $x_0^i \in [-0.3, 0.78]$. Both graphs were calculated over 10^2 iterations after discarding 10^3 transients. Size $N = 10^5$. 26
4.19 Heterogeneous network of pincers maps with $A = 1$, size $N = 10^5$. a) h_t vs. ϵ. b) $\langle\sigma\rangle$ vs ϵ. Initial conditions $x_0^i \in [-0.3, 0.78]$. Both graphs were calculated over 10^2 iterations after neglecting 10^3 iterates. 26
4.20 Pincers map function $f(x) = \left|\tanh(s(x - c))\right|$ as a function of x. The map is singular at the value $x = c$. . . 27
4.21 a) Bifurcation diagram for the pincers map Eq. (4.16) with fixed parameter $s = 1.7$ as a function of c Robust chaos occurs in the interval $c \in [0.25, 0.43]$. For each value of c, 200 iterates are plotted, after discarding 10^3 transient iterations. b) Time series of the pincers map Eq. (4.16) with fixed $s = 1.7, c = 0.25$. 50 iterations are plotted after discarding 10^4 transients. 27
4.22 Network of globally coupled maps Eqs. (4.1) with pincers maps given by Eq. (4.16) with fixed local parameter $s = 1.7$. a)-b) Homogeneous parameters $c_i = 0.25, \forall i$; bifurcation diagram for the mean field h_t vs. ϵ and $\langle\sigma\rangle$ vs. ϵ. c)-d) Maximum heterogeneity $c_i \in [0.25, 0.43]$; bifurcation diagram for the mean field h_t vs. ϵ and $\langle\sigma\rangle$ vs. ϵ. The blue line signals the value $\epsilon = 0.99$. e)-f) Fixed coupling $\epsilon = 0.99$; bifurcation diagram for the mean field h_t and $\langle\sigma\rangle$ vs. the asymmetry parameter A. In all graphs, initial conditions are uniformly distributed on the interval $x_0^i = [-0.19, 0.87]$, system size $N = 10^5$. For each value of ϵ and A, 10^2 iterates are shown, after discarding 10^3 transients. 28
4.23 a) Bifurcation diagram for the mean field h_t and $\langle\sigma\rangle$ vs. the asymmetry parameter A with fixed coupling $\epsilon = 0.99$. b) Magnification of the region of A where collective period five emerges. Blue line signals the value $A = 0.328$. c) Time series of the mean field h_t for the asymmetry value $A = 0.328$. 29
4.24 a) Bifurcation diagram of the map Eq. (4.18) as a function of r. b) Time series dynamics for $r = 2$ over 50 iterations. Both graphs were obtained after discarding 10^4 transients. 30

4.25 a) Bifurcation diagram for the mean field h_t vs ϵ for the homogeneous coupled map network, Eqs. (4.1), with local maps Eq. (4.18) and $r_i = 3$, $\forall i$. The blue vertical line signals the onset of synchronization. b) Mean standard deviation $\langle\sigma\rangle$ vs. ϵ. Initial conditions are in the interval $x_0^i = [0, 1]$. For each value of ϵ, 200 iterations are taken after discarding 10^3 transients. System size $N = 10^5$. 31
4.26 Globally coupled Smooth maps with $\epsilon = 0.7$: a) Bifurcation diagram for the mean field of the network h_t vs A heterogeneity parameter. Initial condition in $x_0^i \in [0, 1]$ and all local parameter values varies from Symmetry state parameters $\mu = 1.1$ to heterogeneous state parameters in $\mu \in [1.1, 4]$. b) Time average standard deviation $<\sigma>$ vs A heterogeneity parameter. Both graphs were calculated over 10^2 iterations after neglecting 10^3 iterates in a system size $N = 10^5$ nodes. 32

Chapter 1

Introduction

In recent years there has been much interest in the study of the collective behavior of networks of coupled dynamical units as models of complex systems. A complex system is a system of interactive elements whose collective behavior is not likely to be derived from the knowledge of the behavior its isolated constituent elements[1,2]. The concept of complex system has become a new paradigm for the search for an unified interpretation of the mechanisms of emergence of structures, patterns, and functionality in a variety of natural and technological systems. Complex systems have been found to possess universal characteristics, regardless of their context. The investigation of the interrelationships between the constituent elements in complex systems has revealed the existence of underlying networks of connectivity which also have universal properties[3].

Synchronization is the simplest and more abundant form of collective behavior arising in systems of interacting elements. Synchronization occurs when all the elements in the system share the same state sustained in time, i.e., the elements reach a common time evolution. Spontaneous or autonomous synchronization can take place without the presence of external fields or driving forces. Synchronization is widely observed in nature, ranging from coupled pendulum clocks, firing of fireflies, the motion of schools of fish, flying flocks, swarms of birds, bees evading predators, in the periodic clapping of hands of people in a stadium, people walking on wobbly bridges, or in epileptic seizures. It has also been artificially designed for technological applications, including wind turbines, satellite clocks, or electrical grid lines[4].

It has generally been assumed that individual entities are more likely to exhibit the same behavior if they are similar to each other, such as animals using the same gait, lasers pulsing together, birds singing the same notes, and social agents reaching consensus. Remarkably, a recent study by Takashi Nishikawa and Adilson Motter[5] demonstrated that this assumption is in fact false for some networks of coupled dynamical units. The mechanism underlying this finding is an instance of a new network phenomenon that has been called *asymmetry-induced symmetry*, in which the collective state of the system can be symmetric only when the elements of system are not.

In their article, Nishikawa and Motter[5] consider the emergence of spontaneous synchronization in a network of N identically-coupled oscillators as a convenient model process to illustrate the core idea of asymmetry-induced symmetry. In this process, the oscillators synchronize by reaching a stable state in which they all exhibit the same dynamics: $x_1(t) = x_2(t) = \cdots = x_N(t)$ for all asymptotic times t. The state of the network then has maximum symmetry, since any two nodes can be swapped without changing the collective synchronized state. It might be intuitive to assume that complete synchronization would require that the oscillators themselves be identical. The rationale for this is that if the oscillators have identical couplings, collective synchronization of the entire network is a macroscopic state inheriting the symmetry of the system only if all of the oscillators are identical. However, Nishikawa and Motter showed the existence of scenarios in which all oscillators synchronize and have identical states if and only if the oscillators themselves are not identical.

Asymmetry-induced symmetry can be interpreted as the converse of the well known phenomenon of symmetry breaking, where the collective state has less symmetry than the elements. Symmetry breaking underlies, for example, the phenomenon of superconductivity, the mechanism through which some elementary particles acquire mass, and various patterns of network dynamics; it also describes several forms of pattern formation, in which initially symmetric or homogeneous structures evolve into asymmetric ones.

1.1 Research problem

The mechanism of asymmetry-induced symmetry has been mainly applied to study synchronization in dynamical systems, since synchronization has long been considered as a paradigm for emergent uniform collective behavior. There are several other collective behaviors that have been studied both theoretically and experimentally in complex dynamical systems, such as generalized synchronization, dynamical clustering, chimera states, and nontrivial collective behavior[6]. We may expect that other forms of collective behaviors may also be related to the existence of heterogeneity or asymmetry in a system. In particular, nontrivial collective behavior consists of the coexistence of ordered evolution of macroscopic variables with chaotic local variables in a system[7]. The research problem in thesis has been motivated by the basic assumption that a process of asymmetry-induced symmetry may be relevant for the emergence of other types of collective behaviors, besides synchronization. A central hypothesis of the present thesis is that the phenomenon of nontrivial collective behavior in chaotic dynamical networks –where collective periodicity arises from local chaos– can be induced by heterogeneity in the constitutive elements of the system.

1.2 Objectives

1.2.1 General objective

Extend the mechanism of asymmetry-induced symmetry, previously investigated in synchronization, to other types of collective behaviors emerging in networks of interacting dynamical elements.

1.2.2 Specific objectives

1. To consider a network of globally coupled maps possessing robust chaos as a simple mathematical model for studying the emergence of nontrivial collective behavior.
2. To define an asymmetry parameter to characterize the degree of heterogeneity in the local parameters on the system.
3. To investigate the occurrence of nontrivial collective behavior as a function of the asymmetry parameter for various systems.
4. To numerically investigate the generality of the phenomenon nontrivial collective behavior induced by asymmetry in a dynamical networks by considering several local maps possessing the property of robust chaos.

In Chapter 2, we present the paper by Nishikawa and Motter and discuss its implications. We provide a short review of the growing literature on this fascinating field. We also briefly describe a recent experimental demonstration of asymmetry-induced symmetry in a network of coupled electronic circuits. Chapter 3 describes the phenomenon of nontrivial collective behavior in homogeneous systems possessing the property of robust chaos. Chapter 4 contains our model of coupled robust chaos map with heterogeneity. We define a heterogeneity parameter and investigate the emergence of collective behaviors as this parameter is varied for several map networks. We report the observation of nontrivial collective behaviors for some ranges of heterogeneity in several systems having different local robust chaos dynamics. We find that nontrivial collective behavior is induced by heterogeneity for values of parameters where the phenomenon does not exist if the system is homogeneous or symmetrical. Conclusions are presented in Chapter 5.

Chapter 2

Theoretical framework: Synchronization induced by asymmetry

In recent years, synchronization has been extensively studied as an emergent collective property in complex systems[4,8]. Synchronization is a phenomenon in which two or more dynamical elements interact with each other resulting in a common evolution of some of their state variables. In many situations, systems are capable of adjusting their pace spontaneously through mutual interactions, showing the same behaviour over time, without external influences. Synchronization phenomena pervades our daily lives. Many of our bodies physiological functions are synchronized to the day-night cycle (circadian rhythm); thousands of pacemaker cells in the sinoatrial node, fire at unison in order to maintain the regular beats of our hearts; thousands of fireflies reunite at night along riverbanks and synchronize their flashes in an amazing spectacle that has been noticed and reported for over three centuries; laser beams are also examples of perfect synchronization of trillions of atoms.

The phenomenon of synchronization can also occur when two or more chaotic systems are coupled. Because of the exponential divergence of trajectories of chaotic systems, having two chaotic systems evolving in synchrony might appear surprising. However, synchronization of autonomous or driven chaotic oscillators is a phenomenon well established both theoretically and experimentally[4].

Synchronization has been observed in networks of interacting homogeneous or symmetrical elements. Synchronization can be considered as collective state of symmetry in a system. It has been long assumed that interacting entities are more likely to exhibit the same behavior if they are identical or very similar, such as pulsating lasers at the same frequency, animals using the same gait, or dynamical systems sharing the same parameters.

In 2016, Takashi Nishikawa and Adilson Motter published a pioneering article titled "Symmetric states requiring system asymmetry" where they demonstrated that this assumption is not necessary[5]. Nishikawa and Motter studied a system where the interacting elements were non-identical. They consider a network of N two-dimensional oscillators, whose dynamics is described by the equations

$$\dot{\theta}_i = \omega + r_i - 1 - \gamma r_i \sum_{j=1}^{N} \sin\left(\theta_j - \theta_i\right), \tag{2.1}$$

$$\dot{r}_i = b_i r_i (1 - r_i) + \varepsilon r_i \sum_{j=1}^{N} A_{ij} \sin\left(\theta_j - \theta_i\right), \tag{2.2}$$

where θ_i y r_i are the angular and amplitude variables for oscillator $i = 1, 2, \ldots, N$, respectively. The parameters ω and $b_i > 0$ characterize the individual dynamics of each oscillator, while the parameters $\gamma > 0$ and $\varepsilon > 0$ represent the coupling strength, and $\mathbf{A} = \left(A_{ij}\right)_{1\leq i,j\leq n}$, with $A_{ij} \geq 0$, is the adjacency matrix that encodes the structure of the network. The influence on a particular oscillator is the sum of the influences from the other oscillators. In particular, they considered the class of uniform networks for which the nodes are arranged in a one-dimensional ring, and each node is coupled to its neighbors. For a given parameter δ, each node i receives an input from node $i-1$ with a coupling strength of $1-\delta$ and from node $i+1$ with a strength of $1+\delta$. Figure 2.1 illustrates the case for $N = 7$.

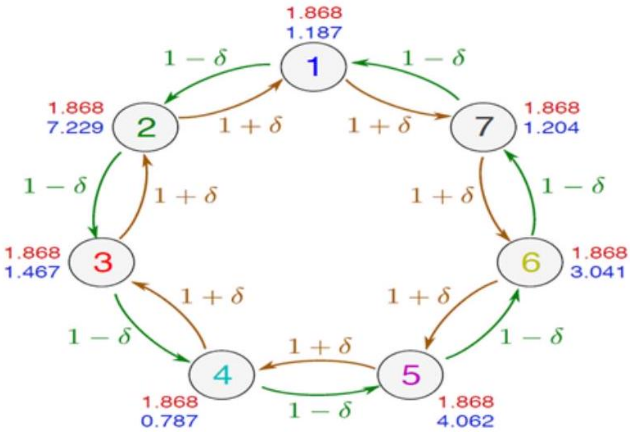

Figure 2.1: 7-node network. The numbers in red and blue are the values of b_i, taken in the simulation, for the cases of homogeneous and heterogeneous distribution in that parameter, respectively.

Nishikawa and Motter found that, for identical values of b_i, the synchronized state ($\theta_1(t) = \cdots = \theta_N(t), r_1(t) = \cdots = r_N(t)$) is unstable. However, when non-identical values of b_i are allowed, the synchronized state can be stable. This type of behavior was called *symmetry induced by asymmetry*. As Figure 2.2 shows, after changing to a combination of inhomogeneous values of b_i for $t \geq 75$, the oscillators spontaneously reach a synchronized state. Nishikawa and Motter point out that while they only considered uniform networks to avoid confounding factors (for example, the differences between oscillators are used to compensate for the differences between their couplings), the conclusion that heterogeneity may be necessary to achieve a common state is general and also valid for non-uniform networks.

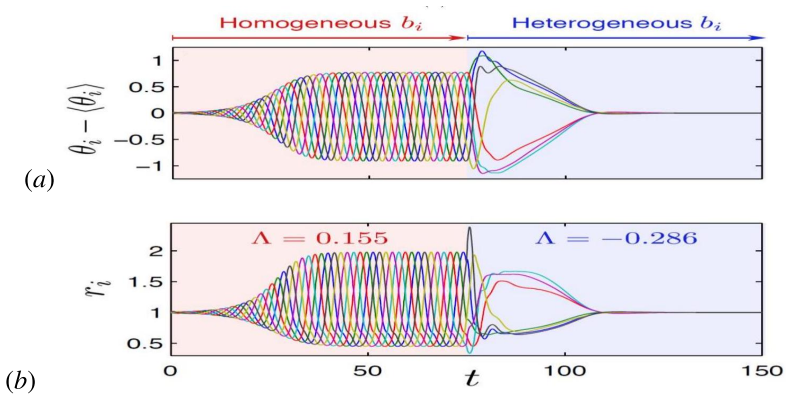

Figure 2.2: Trajectories of the oscillators ($n = 7$). (a) Angular variable θ_i (relative to its average $\langle\theta_i\rangle$) vs t. (b) Amplitud variable r_i vs t. There is a desynchronized state with homogeneous values of $b_i = b^*$ for $t < 75$, followed by spontaneous synchronization with heterogeneity in b_i when $t \geq 75$.

The phenomenon of induced symmetry by asymmetry is a counterintuitive result that challenges the common assumption that identical or similar entities tend to synchronize more easily. Instead, in many systems heterogeneity among

interacting entities may be necessary for synchronization to occur. This has important implications for understanding synchronization in natural and engineered systems, and for developing strategies to control synchronization in such systems. Furthermore, it is not just the existence of a collective symmetric state for an asymmetric system that draws the most attention, but rather the fact that such a state can only be stable when the system is asymmetric.
Y. Zhang, T. Nishikawa, and A. E. Motter have shown experimentally that the asymmetry in the coupling can actually enhance synchronization in a network of coupled Chua's circuits, leading to more symmetric states[9]. An illustration of the experiment is shown in Figure 2.3 from Ref.[10]. This reveals that asymmetry can play a key role in inducing symmetry in networks of non-identical oscillators.

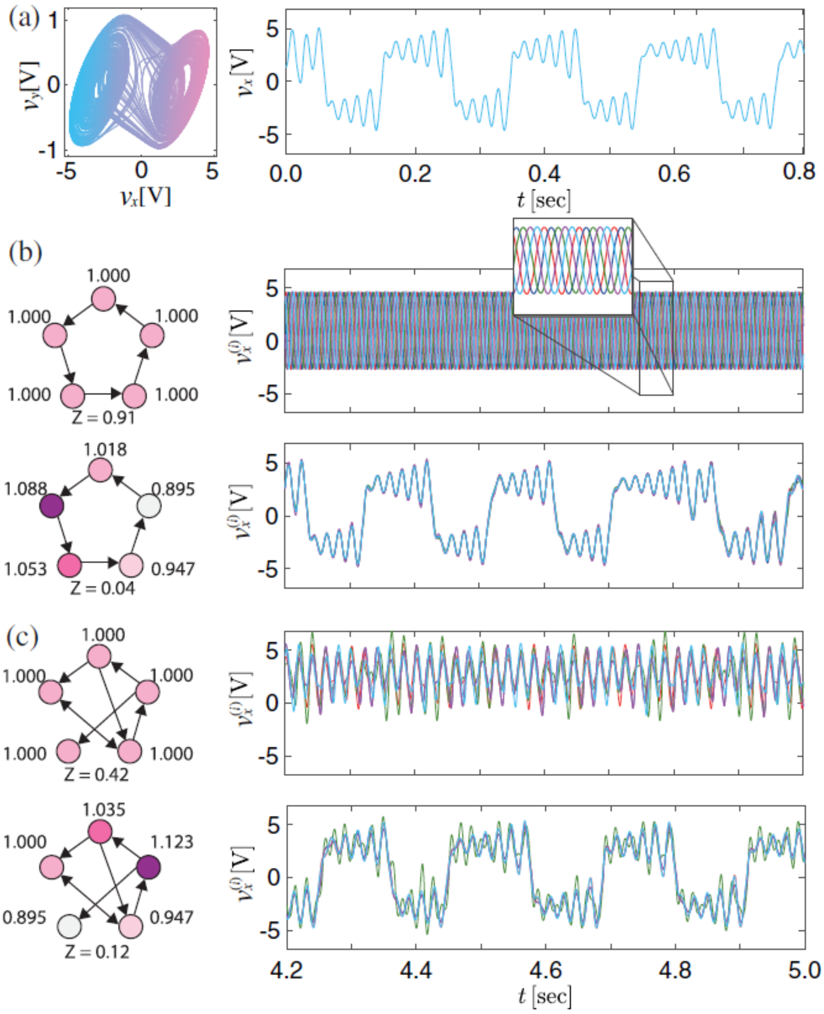

Figure 2.3: Chaos synchronization induced by random oscillator heterogeneity. (a) Double-scroll chaotic attractor constructed from the experimental time series of the voltages V_x and V_y of a single uncoupled oscillator, and the time series for V_x shown separately. (b),(c) Corresponding experimental time series for oscillators in a directed ring for $k = 8.18$ (k controls the coupling strength). (b) and in a random network for $k = 5$. (c). Left: network structures and synchronization errors Z, where each node is labeled with its timescale τ_i. Right: time series after the initial transient (colored by oscillator) for initial conditions close to the synchronous state, showing that chaos synchronization is stable in the heterogeneous system but not in the homogeneous one. In particular, the heterogeneous systems both achieve low synchronization error and preserve qualitative properties of the original chaotic attractor.

Further studies of synchronization in asymmetric and heterogeneous systems has led to significant discoveries in this field. Y. Zhang and A. E. Motter found that the asymmetry-induced symmetry can also play a crucial role in the

emergence of chimera states[11]. Motter and collaborators have shown synchronizing chaos with imperfections[10]. Other authors have found the phenomenon of asymmetry-induced order in multilayer networks[12]. They found that the asymmetry of the network can induce synchronized behavior in the system. Palacios investigated the stability of the synchronization state in networks with homogeneous oscillators that are coupled in an asymmetric manner[13]. It was found that, regardless of whether the network contains homogeneous or heterogeneous oscillators, the synchronization state is stable. Gu et al.[14] demonstrated that the heterogeneity in the properties of neurons can induce synchronized behavior in the brain. These results suggest that the synchronization of oscillators in asymmetrically coupled networks is a robust phenomenon that can arise even in the presence of an asymmetry in the system.
In summary, in recent years it has been revealed that synchronization is an emergent property of complex systems that can be induced by both symmetry and asymmetry in the system. This phenomenon have significant implications for various fields such as neuroscience, biology, physics, engineering, and social sciences. The understanding of synchronization in complex systems is crucial for the development of new technologies and the advancement of interdisciplinary science. Furthermore, synchronization in neural networks plays an important role in the functioning of the brain and has been extensively studied in neuroscience, highlighting the importance of this research in the field. Asymmetry-induced symmetry may have implications in other collective behaviors. For example, it offers a mechanism for convergent forms of pattern formation where an asymmetric structure develops into a symmetric one, such as in the development of fivefold radial symmetry in starfish from bilateral symmetry in starfish larvae. A can also have implications for social dynamics, potentially yielding scenarios in which interacting agents only reach consensus when they are different from each other; this means that diversity may facilitate, and even be required for, consensus of opinions.
The discovery of synchronization induced by asymmetry has motivated the present investigation: the search for other collective behaviors, besides synchronization, that may be induced by the presence of asymmetry or heterogeneity in a dynamical system.

Chapter 3

Nontrivial collective behaviour in globally coupled map networks

There exist systems in nature that exhibit collective behaviors that are not susceptible of being inferred from the behavior of their isolated constituent elements. The collective behavior is said to emerge from the interactions between the elements. These systems have been denoted as complex systems. Emergent properties, sharing the same characteristics, arise in physical, chemical, biological, and social systems. In networks of dynamical elements, the investigation of collective behavior has fundamental implications for the understanding of universal properties observed in complex systems. An interesting collective phenomenon consists of an ordered evolution of macroscopic variables of the system arising out of local chaos. This phenomenon is known as nontrivial collective behavior[7,15–17].
Nontrivial collective behavior can be observed in simple dynamical systems such as coupled map networks. Coupled map lattices or coupled map networks are spatiotemporal dynamical systems where space and time are discrete, but the state variables are continuous. They consist of a set of maps, or iterative functions, considered as nodes interacting on a lattice or on a general network[18–21]. Coupled map networks have provided useful models for the study of diverse spatiotemporal processes in spatially extended systems, with the advantage of being computationally efficient and, in some cases, mathematically tractable.
In this context, globally coupled map networks, where each element interacts with each other in the system, constitute paradigmatic models for the current research of complex systems that possess global interactions[22]. A global interaction occurs when all the elements in the system are subject to the same influence or share the same information. Many physical, chemical, biological, social, and economic systems are subject to global interactions. Global interactions can provide useful descriptions in networks possessing highly interconnected elements or long-range interactions. The origin of a global interaction can be either external, as in a forcing field; or autonomous, such as a mean field or a feedback coupling function that depends on the elements of the system[23,24]. Global interactions appear, for example, in parallel electric circuits, coupled oscillators[25,26], charge density waves[27], Josephson junction arrays[28], multimode lasers[29], neural networks, evolution models, ecological systems[2], social networks[30], economic exchange[31], mass media influence[32–34], and cultural globalization[35]. A complete graph, where any node can interact each each other, can be seen as a global interaction. Diverse collective behaviors have been observed experimentally in globally coupled oscillators, such as complete and generalized chaos synchronization, dynamical clustering, nontrivial collective behavior, chaotic itinerancy, quorum sensing, and chimera states[36–41]. A globally coupled map system that can be defined as follows[16,42],

$$x_{t+1}^{i} = (1-\epsilon) f(x_t^i) + \frac{\epsilon}{N} \sum_{j=1}^{N} f(x_t^j) \tag{3.1}$$

where x_t^i, $i = 1, 2, \ldots, N$, is the state of the ith element at discrete time $t = 0, 1, 2, \ldots$, N is the size of the system; ϵ is a parameter expressing the strength of the coupling, and the function $f(x_t^i)$ describes the local dynamics that may depend on some parameters. The global interaction occurs through the mean field of the system, however other forms of coupling functions can be employed, as long as they are shared by all the elements. The coupling scheme in Eqs. (3.1) is called diffusive, because it corresponds to the discrete form of the Laplacian operator in a diffusion equation. Figure (3.1) illustrates a globally coupled network system.

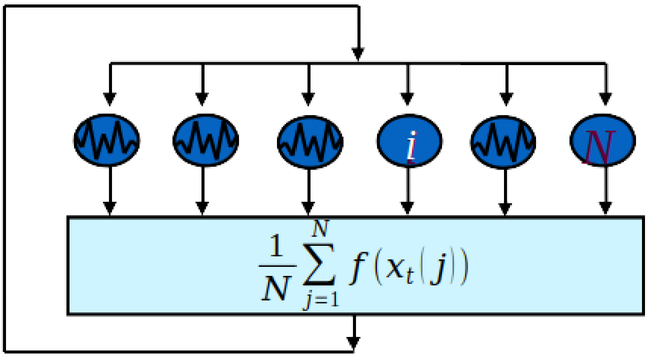

Figure 3.1: Schematic representation of a globally coupled map network described by Eqs. (3.1).

As an example of the phenomenon of nontrivial collective behavior, consider, as local dynamics, the logarithmic map [16]

$$x_{t+1} = f(x_t) = b + \ln |x_t|, \tag{3.2}$$

where b is a real parameter. This map exhibits robust chaos, with no periodic windows, on the interval $b \in [-1, 1]$. A chaotic attractor is said to be robust if, for its parameter values, there exist a neighborhood in the parameter space with absence of periodic windows and the chaotic attractor is unique. Robustness is an important property in applications that require reliable operation under chaos, in the sense that the chaotic behavior cannot be destroyed by arbitrarily small perturbations of the parameters of the system. Figure (3.2) shows the bifurcation diagram of x_t as a function of b for the logarithmic map (From Ref. [16]).

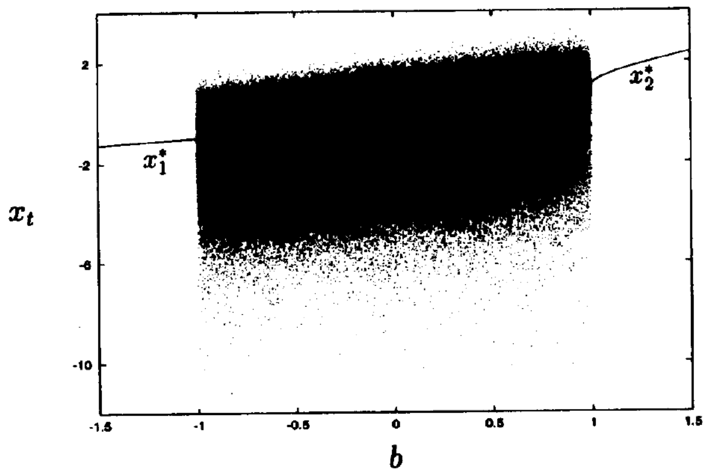

Figure 3.2: Bifurcation diagram of the logarithmic map Eq. (3.2) as a function of the parameter b. Robust chaos occur for $b \in [-1, 1]$. x_1^* for $b < -1$ and x_2^* for $b > 1$ are fixed points. For each value of b, 100 iterates are shown, after discarding 1000 transient points.

As a statistical quantity characterizing the collective behavior for the system Eq. (3.1), we consider the mean field

$$h_t = \frac{1}{N}\sum_{j=1}^{N} f(x_t^j). \tag{3.3}$$

Figure (3.3) shows the evolution in time of both, the quantity h_t and one local map in the globally coupled system Eqs. (3.1) for given values of parameters b and ϵ. We observe a periodic motion (period two) of the macroscopic variable h_t coexisting with the local chaotic dynamics. This is an instance of nontrivial collective behavior.

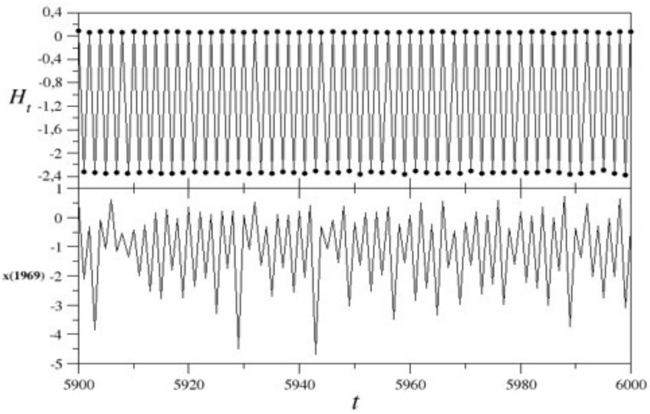

Figure 3.3: Top: Time-evolution of the mean field h_t, Eq. (3.3), for the globally coupled system Eqs. (3.1), showing period two motion. Bottom: Time-evolution of the local map x^{1969} in the system Eqs. (3.1 exhibiting chaotic dynamics. Random initial conditions on the maps, uniformly distributed on the interval $x_0^i \in [-8, 4]$ are used for the globally coupled system Eqs. (3.1). Parameters for the system Eqs. (3.1) are $b = -0.7$, $\epsilon = 0.2$, $N = 10^5$.

Nontrivial collective behavior can occur for a range of parameters in a system. Figure (3.4) (from Ref. [16]) shows the bifurcation diagram of the mean field h_t as a function of the parameter b, with a fixed value of the coupling ϵ. For values of the parameter b in the interval $[-1, 1]$, the elements x_t^i are locally chaotic and desynchronized. However, the mean field h_t displays a collective periodic behavior coexisting with local chaos.

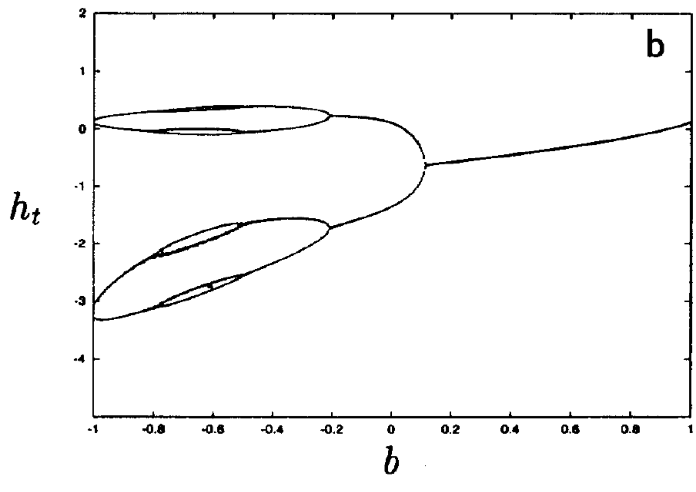

Figure 3.4: Bifurcation diagram of the mean field h_t, Eq. (3.3), for the globally coupled system Eq. (3.1) as a function of the parameter b with fixed coupling $\epsilon = 0.25$. Size of the system $N = 10^5$. For each value of b, h_t is calculated for 100 time steps during a run starting from random initial conditions on the maps, uniformly distributed on the interval $x_0^i \in [-8, 4]$, after discarding 1000 transients.

Figure (3.5) from ref.[16] shows the bifurcation diagram of the mean field h_t as a function of the coupling parameter ϵ, with a fixed value of the parameter b of the local maps. Again, collective periodic orbits (period 2, 4, 8) appear for some intervals of the coupling parameter ϵ.

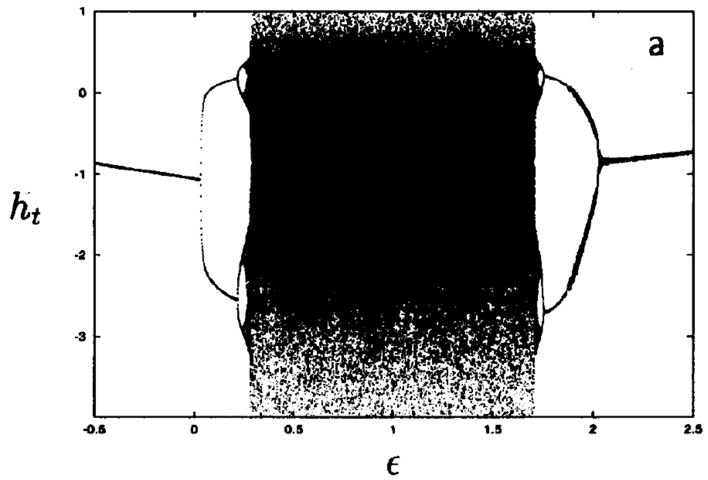

Figure 3.5: Bifurcation diagram of the mean field h_t, Eq. (3.3), for the globally coupled system Eqs. (3.1) as a function of the coupling parameter ϵ, with a fixed value of the parameter $b = -0.7$ for the local maps. Size of the system $N = 10^5$. Random initial conditions are used for each value of ϵ, as in Fig. (3.4).

Note that the periodic behavior in the macroscopic quantity h_t appears for values of the parameter b where the isolated logarithmic maps possess robust chaos. The mean field h_t displays orbits of periods 2, 4, 8, 16, as a function of the coupling parameter ϵ, similar to the period-doubling bifurcation characteristic of smooth unimodal maps (possessing a single maximum or minimum). However, the local logarithmic map is singular, it does not possesses any periodicity on the interval $b \in [-1, 1]$, and it does not belong to the universal class of smooth unimodal maps. Thus, the mean field h_t has acquired properties that are not present in the local logarithmic maps. The periodicity arising in the mean field of the system cannot be attributed to the existence of stable periodic orbits in the local maps. Therefore, the periodic, ordered behavior of the mean field is a emergent nontrivial collective property of the system Eqs. (3.1).
In next chapter, we investigate globally coupled networks of coupled heterogeneous logarithmic maps, as well as several other networks possessing heterogeneous local maps. Heterogeneity is added to those systems through an asymmetry parameter that we introduce in this thesis.

Chapter 4

Heterogeneous dynamical networks: Results

4.1 Heterogeneity/Asymmetry parameter

In this Chapter, we present the model proposed in this thesis to investigate other manifestations of collective behavior that may be induced by asymmetry in dynamical networks, besides the phenomenon of asymmetry-induced synchronization discovered by Nishikawa and Motter.

We introduce asymmetry in parameters of the local elements that constitute a network. As a simple model, we shall consider a globally coupled map model with heterogeneous parameters for the local maps, in the form

$$x_{t+1}^{i} = (1-\epsilon) f(x_t^i, r_i) + \frac{\epsilon}{N} \sum_{j=1}^{N} f(x_t^j, r_j), \tag{4.1}$$

where $f(x_t^i, r_i)$ is a function that represents the local dynamics that can take different parameter values $r_i \in [R_1, R_2]$ for each element i, $i = 1, 2, \ldots, N$. Here we consider intervals $[R_1, R_2]$ where the map $f(x_t)$ exhibits robust chaos. Then, any occurrence of nontrivial collective behavior in the heterogeneous system Eqs. (4.1) may not be attributed to the presence of local windows of periodicity in the local dynamics. As in the previous chapter, the parameter ϵ expresses the intensity of the coupling between the elements. Here we consider that the coupling strength is homogeneous; heterogeneity occurs only in the local dynamics.

When the local map parameters r_i are all identical, the system is homogeneous or symmetrical, i.e., $r_i = r_j$, $\forall i, j$, which corresponds to the globally coupled systems that have been extensively studied before. Instead, here the parameter r_i can be in the robust chaos interval $[R_1, R_2]$ of the map f, so that in general, $r_i \neq r_j$. We introduce a control parameter $A \in [0, 1]$ to characterize the amount of asymmetry or heterogeneity in the system, by assigning the individual parameters r_i according to the rule

$$r_i = R_1 + A\,\xi\,(R_2 - R_1), \tag{4.2}$$

where $\xi = \text{random}[0, 1]$ is a random number generated between 0 and 1 with uniform probability. There are many random number generators available that fulfill this statistical property. Then, when $A = 0$, we have $r_i = r_j$, $\forall i$, and the elements are homogeneous. When, $A = 1$, the parameter r_i can take any value in the interval $[R_1, R_2]$ and we have maximum heterogeneity. In this way, for a given value of A, the parameters r_i will be distributed uniformly at random in the sub-interval

$$r_i \in [R_1, R_1 + A(R_2 - R_1)], \quad \forall i. \tag{4.3}$$

Thus, the quantity A defines the width of the sub-interval in $[R_1, R_2]$ where the parameters r_i are distributed. Therefore,

we call A the asymmetry parameter that measures the degree of heterogeneity of the system. In Eq. (4.2), heterogeneity is defined as a deviation from the parameter value R_1 considered as homogeneous, but any other value of r in the interval $[R_1, R_2]$ can be considered as the homogeneous value about which a random distribution of the parameters r_i can be performed.
In addition, synchronization in a coupled map network at time t can be characterized by the instantaneous standard deviations of the distributions of the state variables, defined as

$$\sigma_t = \left[\frac{1}{N}\sum_{i=1}^{N}\left(x_t^i - \bar{x}\right)^2\right]^{1/2}, \tag{4.4}$$

where

$$\bar{x} = \frac{1}{N}\sum_{j=1}^{N} x_t^j. \tag{4.5}$$

We define the mean standard deviation $\langle\sigma\rangle$ as a statistical quantity to characterize a collective synchronization state in a coupled map network, by the asymptotic time average

$$\langle\sigma\rangle = \frac{1}{T}\sum_{t=\tau}^{\tau+T}\sigma_t, \tag{4.6}$$

where τ is a number of discarded transients and T is a sufficient large iteration step. Synchronization in a system at time t happens when $x_t^i = \bar{x}, \forall i$. Then, a stable collective synchronization state arises when $\langle\sigma\rangle = 0$. For numerical calculations we shall consider $\langle\sigma\rangle < 10^{-8}$ as a synchronization condition.

4.2 Non-trivial collective behaviour induced by heterogeneity

4.2.1 Heterogeneous network of logarithmic maps

We recall the dynamics of a single, uncoupled logarithmic map, given by

$$x_{t+1} = f(x_t) = \ln|x_t| + b. \tag{4.7}$$

For values of the parameter $b \in [-1, 1] = [R_1, R_2]$, this map exhibits robust chaos [16]. Figure 4.1 shows the bifurcation diagram $f(x_t)$ as a function of b for the logarithmic map Eq. (4.7)

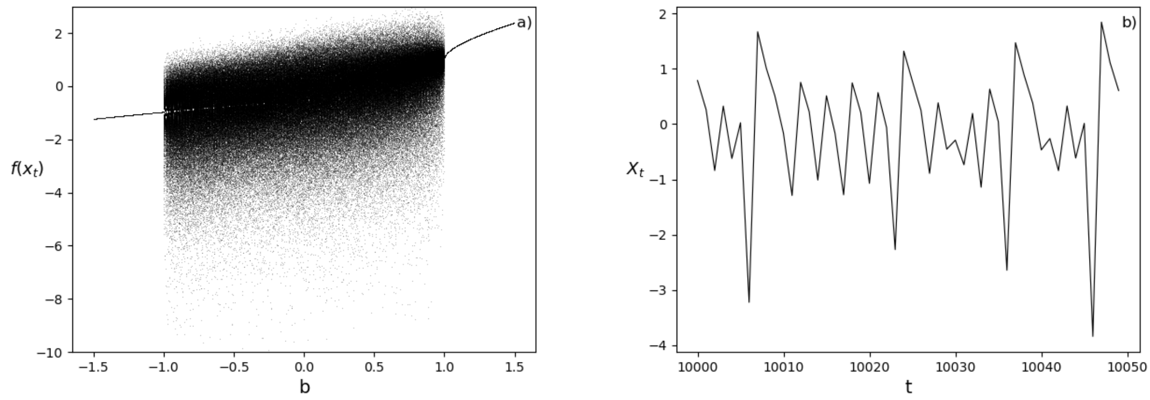

Figure 4.1: a) Bifurcation diagram logarithmic map Eq. (4.7) showing robust chaos in $b \in [-1, 1]$. For each value of b, 200 iterations are plotted after discarding 10^4 transients. b) Time series for 50 iterations, after discarding 10^4 iterations, for the logarithmic map with $b = 0.5$.

Homogeneous parameters

We first consider a globally coupled map network

$$x_{t+1}^i = (1-\epsilon) f(x_t^i, b) + \frac{\epsilon}{N} \sum_{j=1}^{N} f(x_t^j, b), \tag{4.8}$$

with homogeneous local dynamics given by the logarithmic map Eq. (4.7) with $b = b_i = -0.7$. The collective behavior of the homogeneous network Eq. (4.8) is shown through the mean field h_t and the mean standard deviation $\langle\sigma\rangle$ as functions of the coupling ϵ in Fig. (4.2).

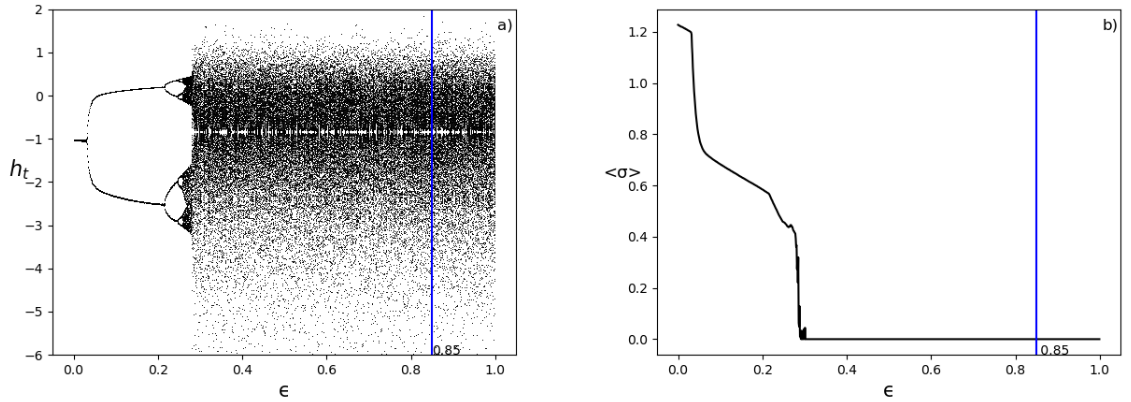

Figure 4.2: Globally coupled Logarithm maps. a) Bifurcation diagram for the mean field of the homogeneous network h_t as a function of the coupling parameter ϵ. b) Time average standard deviation $\langle\sigma\rangle$ vs. ϵ. In both graphs, initial conditions are uniformly distributed on the interval $x_0^i = [-8, 4]$, system size $N = 10^5$, and local parameters were fixed at $b = -0.7$. For each value of ϵ, 10^2 iterates are shown after discarding 10^3 transients. The vertical blue line signals the value $\epsilon = 0.85$.

Figure (4.2)a reveals the emergence of nontrivial collective behavior on an interval of ϵ in the form of periodic orbits for the mean field h_t. Figure (4.2)b shows that the homogeneous network Eq. (4.8) reaches collective synchronization characterized by $\langle\sigma\rangle = 0$ above some critical value of the coupling parameter ϵ.

Asymmetry-induced nontrivial collective behavior

As an application of our heterogeneous model, we consider a globally coupled map network

$$x^i_{t+1} = (1-\epsilon) f(x^i_t, b_i) + \frac{\epsilon}{N}\sum_{j=1}^{N} f(x^j_t, b_j), \tag{4.9}$$

with local dynamics given by the logarithmic maps,

$$f(x^i_t) = \ln|x^i_t| + b_i, \tag{4.10}$$

where the local parameters b_i are distributed in the interval $[R_1, R_2]$ with $R_1 = -1, R_2 = 1$, according to Eq. (4.2) as

$$b_i = -1 + 2A\,\xi. \tag{4.11}$$

Figure (4.3)a shows the bifurcation diagram of the mean field h_t as a function of the asymmetry parameter A for the heterogeneous network Eq. (4.9) with a fixed coupling parameter value $\epsilon = 0.85$. For $A = 0$ we have a homogeneous network of logarithmic maps with $b_i = -1$, $\forall i$, where no collective periodicity exists and the system is synchronized ($\langle\sigma\rangle = 0$). As A increases, periodic windows emerge. As $A \to 1$, a period-3 windows appears. Thus, nontrivial collective behavior is induced by asymmetry in the parameters. Note that increasing the asymmetry A increases the desynchronization in the system as seen in Fig. (4.3)b. Nontrivial collective behavior emerges when the system is desynchronized.

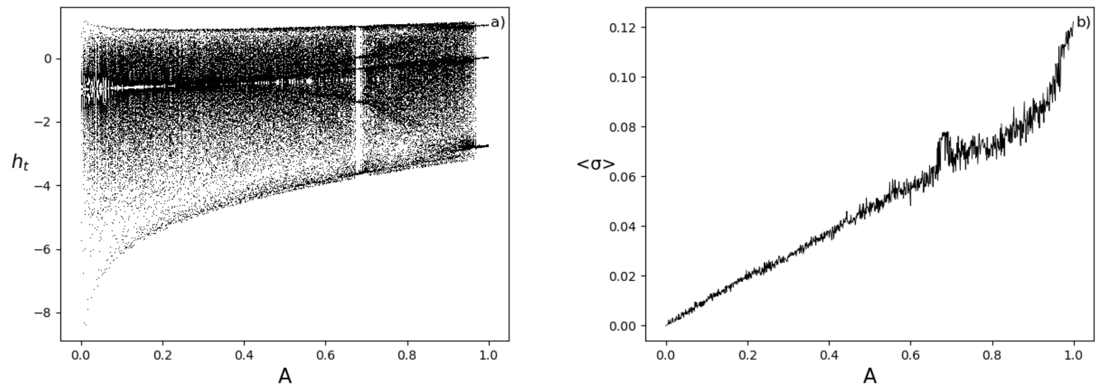

Figure 4.3: a) Bifurcation diagram for the mean field of the network h_t vs. the asymmetry parameter A. b) Mean standard deviation $\langle\sigma\rangle$ as a function of the asymmetry parameter A. Fixed parameters are $\epsilon = 0.85$, size $N = 10^5$. For each value of A, 10^2 iterates are shown after discarding 10^3 transients. Initial conditions $x^i_0 \in [-8, 4]$.

Maximum heterogeneity

Figure (4.4) shows the bifurcation diagram of the mean field h_t and the quantity $\langle\sigma\rangle$ as functions of ϵ for the heterogeneous network system Eq. (4.9) with maximum asymmetry parameter value $A = 1$. We see in Fig. (4.4)a that heterogeneity in the local parameters does not destroy the periodic collective behavior. Furthermore, the asymmetry in the parameters produce windows of periodic collective behavior that were not present in the homogeneous system, Figure (4.2)a. Note that the heterogeneous system does not synchronize in Fig. (4.4)b, in contrast to the homogeneous case Fig. (4.2)b.

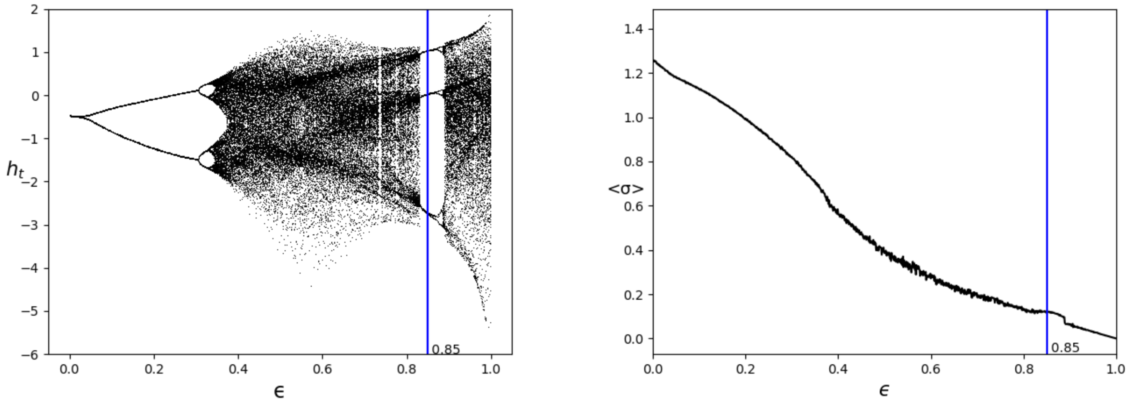

Figure 4.4: a) Bifurcation diagram h_t vs ϵ for the mean field of the maximum heterogeneous logarithmic map network, Eq. (4.9). b) $\langle\sigma\rangle$ vs ϵ. In both graphs, initial conditions are uniformly distributed on the interval $x_0^i = [-8, 4]$, system size $N = 10^5$, and local parameters are uniformly distributed at random $b_i \in [-1, 1]$ corresponding to $A = 1$. For each value of ϵ, 10^2 iterates are shown after discarding 10^3 transients. The vertical blue line signals the value $\epsilon = 0.85$.

Remarkably, the mean field h_t of the fully heterogeneous network exhibits a period-3 collective motion on a range of ϵ. *As far as we know, nontrivial collective orbits with odd periods have not been reported before*. Figure (4.5) shows the time evolution of h_t for the coupling parameter value $\epsilon = 0.85$, showing the collective period-3 motion, although the local maps have parameters in the robust chaos range $[-1, 1]$.

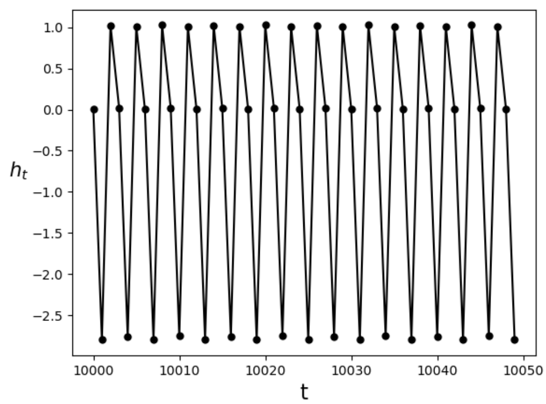

Figure 4.5: Time series of the mean field h_t shows period three for the value $\epsilon = 0.85$ marked in Fig. (4.4). 50 iterations are shown after discarding 10^4 steps.

These results provide evidence that asymmetry can induce collective behaviors in dynamical networks, other than synchronization.

In order to explore the generality of this phenomenon, in the following we shall investigate coupled map networks with different heterogeneous local dynamics possessing robust chaos.

4.2.2 Heterogeneous network of singular maps

Next, consider the globally coupled network with heterogeneous maps given by

$$x_{t+1}^i = (1-\epsilon) f(x_t^i, \mu_i) + \frac{\epsilon}{N} \sum_{j=1}^{N} f(x_t^j, \mu_j), \tag{4.12}$$

with local dynamics given by the singular maps[43],

$$f(x_t, \mu_i) = \mu_i - |x_t|^z, \tag{4.13}$$

with $|z| < 1$, where the local parameters are distributed on an interval $\mu_i \in [\mu_-(z), \mu_+(z)]$ that depends on z, as shown in Fig4.7, according to

$$\mu_i = \mu_-(z) + A\,\xi\,(\mu_+(z) - \mu_-(z)). \tag{4.14}$$

For $|z| < 1$, these maps possess a positive Schwarzian derivative[44] and thus they do not belong to the family of unimodal maps with $|z| > 1$ that show period-doubling. The exponent z describes the order of the singularity at the origin. These maps are unbounded and exhibit robust chaos on a single interval of the parameter μ that depends on z. These maps were employed to characterize the transition to chaos via intermittency in Ref.[43]. The logarithmic map belongs to this family of singular maps.

Figure (4.6)a shows the bifurcation diagram of a single singular map with $z = -0.25$. There exist robust chaos, with no periodic windows, in the interval $\mu \in [0.98, 1.64] = [R_1, R_2]$ for this value of z. The time series of the map corresponding to the parameter value $\mu = 1.1$ is shown in Fig (4.6)b.

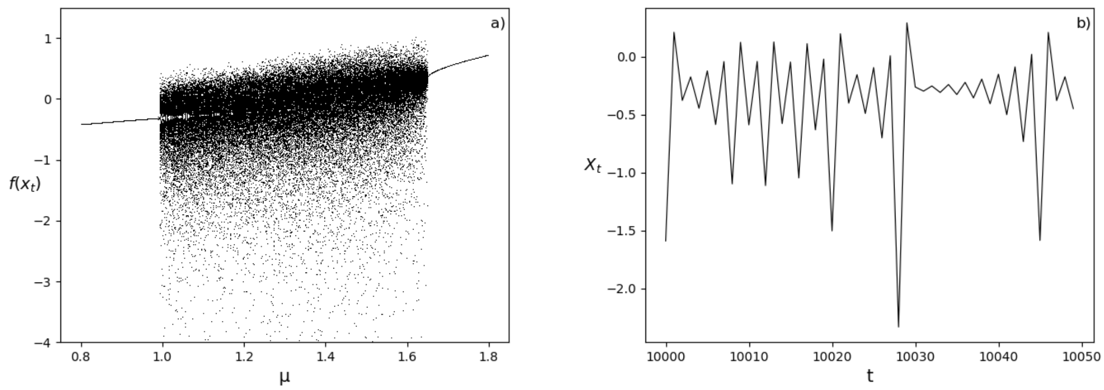

Figure 4.6: a) Bifurcation diagram of a singular map with $z = -0.25$ as a function of the parameter μ. For each value of μ, 100 iterations are shown after discarding 10^4 iterates . b) Chaotic time series of x_t for $z = -0.25$ and fixed $\mu = 1.1$ after discarding 10^4 iterates.

Figure (4.7) from ref[43] shows the dynamical properties of the family of singular maps on the space of parameters (μ, z), with $|z| < 1$.

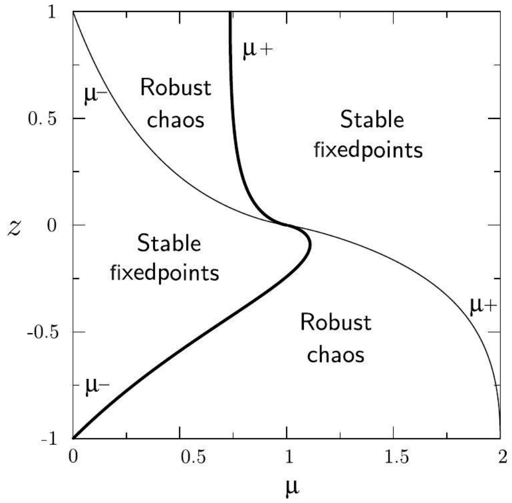

Figure 4.7: Critical boundaries $\mu_-(z)$ and $\mu_+(z)$ of the robust chaos region for the singular maps on the space of parameters (μ, z).

Homogeneous parameters

A symmetric, homogeneous network of coupled singular maps Eqs. (4.12) is obtained when $\mu_i = \mu$, $\forall i$. We choose a singularity exponent fixed at $z = -0.25$ and a homogeneous local parameter $\mu = 1.1$, where there exist robust chaos. Figure (4.8) shows the mean field h_t and mean standard deviation $\langle\sigma\rangle$ as functions of the coupling strength ϵ.

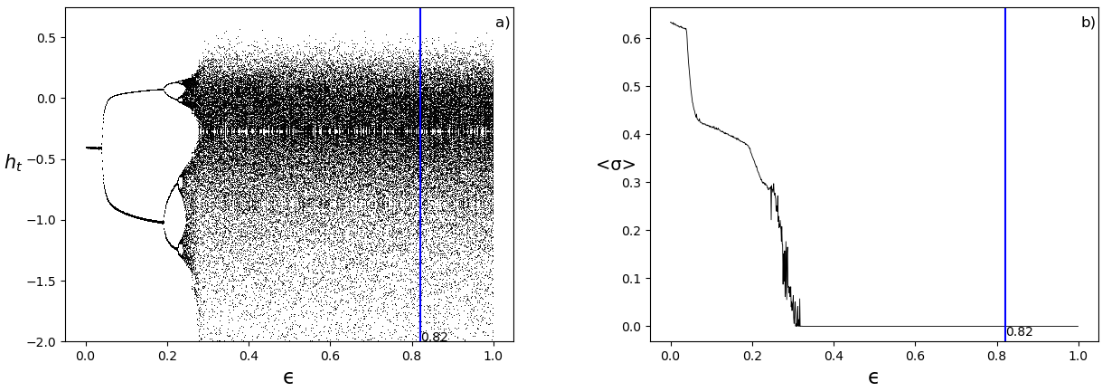

Figure 4.8: Globally coupled homogeneous singular maps Eqs. [4.12] with $z = -0.25$ and $\mu_i = 1.1$. a) Bifurcation diagram h_t vs ϵ. b) Mean standard deviation $\langle\sigma\rangle$ vs ϵ. In both graphs, initial conditions are uniformly distributed on the interval $x_0^i = [-8, 2]$, system size $N = 10^5$. For each value of ϵ, 10^2 iterates are shown after discarding 10^3 transients. The vertical blue line signals the value $\epsilon = 0.82$.

In Fig.(4.8)a, we see that, despite the chaotic behavior of the local maps, for a range of values of the coupling parameter ϵ, the dynamics of the mean field is periodic. Nontrivial collective behavior occurs when the system is desynchronized. Figure (4.8)b shows that the homogeneous system synchronizes ($\langle\sigma\rangle = 0$) above some critical value of the coupling ϵ. Figure (4.9)a shows the time series of the mean field h_t exhibiting period two, while a local map in the network follows a chaotic behavior as seen in Fig.(4.9)b. Then, the homogeneous system of coupled singular maps shows nontrivial collective behavior for some range of parameters.

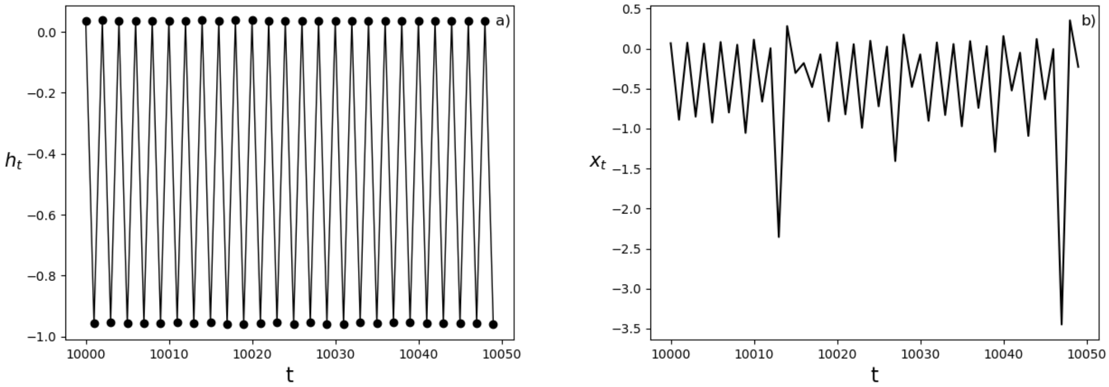

Figure 4.9: a) Time evolution of the mean field h_t for the homogeneous system Eqs. [4.12] with $z = -0.25$ and $\mu = 1.1$ and the coupling value $\epsilon = 0.1$ displaying period-two collective behaviour. b) Time evolution of one map in the network displaying chaotic dynamics coexisting with the collective periodic behavior.

Asymmetry-induced nontrivial collective behavior

Consider the network of coupled singular maps Eqs. (4.12) with fixed coupling $\epsilon = 0.82$, local maps with $z = -0.25$ and parameters μ_i distributed in the robust chaos range $[R_1, R_2] = [0.98, 1.64]$ according to Eq. (4.14) as

$$\mu_i = 0.98 + A\,\xi\,(1.64 - 0.98). \tag{4.15}$$

Figure (4.10)a shows the bifurcation diagram of the mean field h_t as a function of the asymmetry parameter A. When $A = 0$, the system is homogeneous with the uniform local parameter value $\mu_i = 0.98$, $\forall i$. In this case, no periodic collective behavior exists in the system. As A is increased, nontrivial periodic windows are induced in the mean field h_t. For $A \to 1$, the system is fully heterogeneous. Figure (4.10) shows that increasing the asymmetry parameter A takes the system away from synchronization.

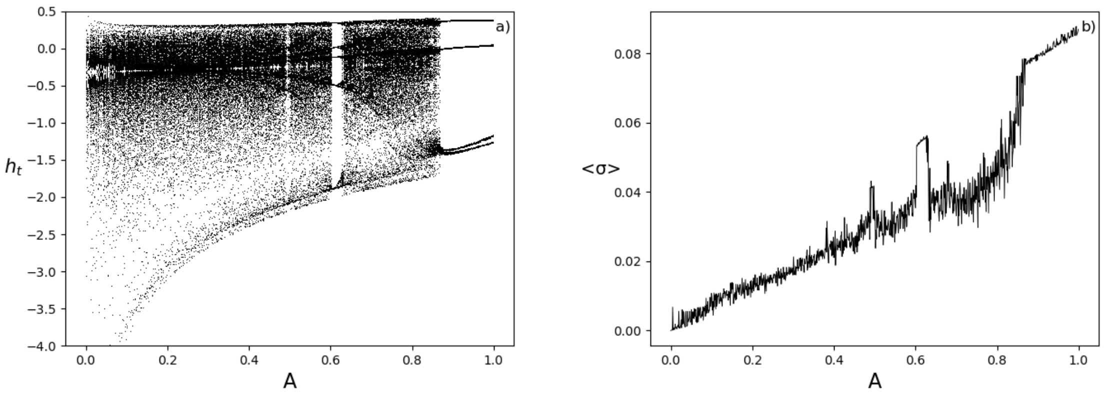

Figure 4.10: a) Bifurcation diagram for the mean field h_t as a function of the asymmetry parameter A for the network of coupled singular maps Eqs. (4.12) with fixed coupling $\epsilon = 0.82$ and local maps with $z = -0.25$. b) Mean standard deviation $\langle\sigma\rangle$ vs. A. In both graphs, initial conditions are uniformly distributed on the interval $x_0^i = [-8, 2]$, system size $N = 10^5$. For each value of A, 10^2 iterates are shown after discarding 10^3 transients.

The heterogeneity/asymmetry parameter A allows for the exploration of collective dynamics that can lead to nontrivial emergent behavior that does not occur in when the system is homogeneous. It is important to note that, due to the different collective dynamics that arise as a function of A, the asymmetry parameter can be treated as a bifurcation parameter for the network collective field dynamics, providing a new way to study collective behavior from homogeneous to heterogeneous complex networks. It should be noted that robust chaotic domains are used, so the non-trivial collective behavior cannot be attributed to periodic windows that may occur in any of the elements, leaving heterogeneity or asymmetry in the parameters as the direct cause of this phenomenon.
As we have mentioned, collective periodic dynamics with odd-periods have not been reported before, as far as we have investigated. Thus, it is interesting to find that the mean field h_t exhibits period-five behavior when the asymmetry parameter takes the value of $A = 0.609$, as depicted in Fig.(4.11)a. Note that the system is not synchronized in Fig.(4.11).

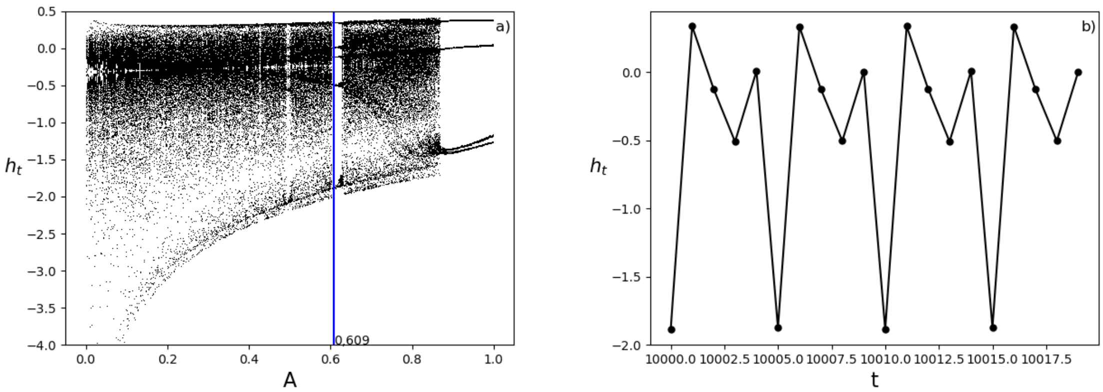

Figure 4.11: a) Bifurcation diagram for the mean field h_t as a function of the asymmetry parameter A for the network of coupled singular maps Eqs. (4.12) with fixed coupling $\epsilon = 0.82$ and local maps with $z = -0.25$. System size $N = 10^5$. b) Period-five collective behavior of h_t when $A = 0.609$, calculated over 20 iterations after discarding 10^4 transients.

Similarly, Fig. (4.12)a shows the bifurcation diagram of the mean field h_t as a function of the asymmetry parameter A for the network of coupled singular maps Eqs. (4.12) with fixed coupling $\epsilon = 0.89$ and local maps with $z = -0.25$. Both, the homogeneous system with $A = 0$ and the fully heterogeneous system with $A = 1$, exhibit collective chaotic dynamics. Now a window of period-three collective behavior emerges on an intermediate range of the asymmetry parameter A. Figure (4.12)b shows the period-three time series of the mean field h_t for the asymmetry parameter value $A = 0.809$.

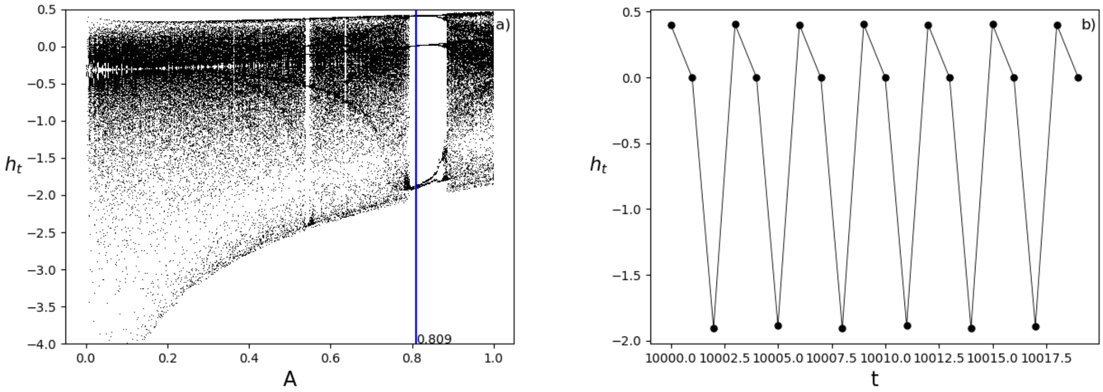

Figure 4.12: a) Bifurcation diagram for the mean field h_t as a function of the asymmetry parameter A for the network of coupled singular maps Eqs. (4.12) with fixed coupling $\epsilon = 0.89$ and local maps with $z = -0.25$. The blue line signals the value $A = 0.809$. System size $N = 10^5$. b) Time series period-three collective behavior of h_t for the asymmetry parameter $A = 0.809$, calculated over 20 iterations after discarding 10^4 transients.

Maximum heterogeneity

Figure (4.13) shows the bifurcation diagram of the mean field h_t and the mean standard deviation $\langle\sigma\rangle$ as functions of ϵ for the network of coupled singular maps Eqs. (4.12) with $z = -0.25$ with maximum asymmetry parameter value $A = 1$. The mean field shows nontrivial collective behaviour with a period-doubling window and a period-six window, as showed in Fig.(4.13)a.

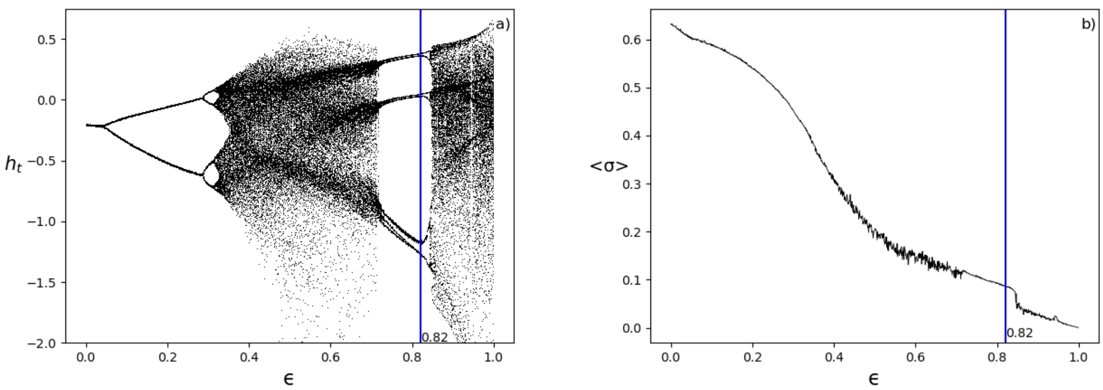

Figure 4.13: Globally coupled singular maps Eqs. [4.12] with $z = -0.25$ and maximum heterogeneity $A = 1$, corresponding to the local parameters distributed in the robust chaos range $\mu_i \in [0.98, 1.64]$. a) Bifurcation diagram h_t vs ϵ. b) Mean standard deviation $\langle\sigma\rangle$ vs ϵ. In both graphs, initial conditions are uniformly distributed on the interval $x_0^i = [-8, 2]$, system size $N = 10^5$. For each value of ϵ, 10^2 iterates are shown after discarding 10^3 transients. The vertical blue line signals the value $\epsilon = 0.82$.

Other singular exponents z

Next, we explore the influence of the exponents of the singular maps, Eq. (4.13). Figure (4.14)a shows the bifurcation diagram of a single singular map with exponent $z = 0.5$ as a function of μ. Robust chaos appears in the interval

$\mu \in [0.25, 0.75]$, with two chaotic bands. Figure (4.14)b shows the time series of x_t for the parameter value $\mu = 0.5$.

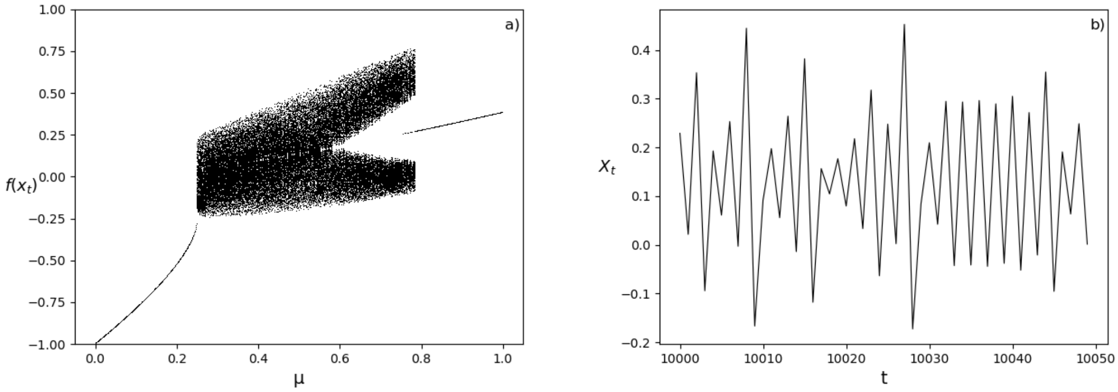

Figure 4.14: a) Bifurcation diagram of a singular map with $z = 0.5$ as a function of μ. For each value of μ, 100 iterates are shown, after discarding 10^5 transients iterations. b) Time series of x_t for the parameter value $\mu = 0.5$, calculated over 50 iterations after discarding 10^4 transients.

Figure (4.15) shows bifurcation diagrams of the mean field h_t and the mean standard deviation $\langle\sigma\rangle$ for the homogeneous, fully heterogeneous, and asymmetry-dependent network of coupled singular maps Eqs. (4.12) with $z = 0.5$.

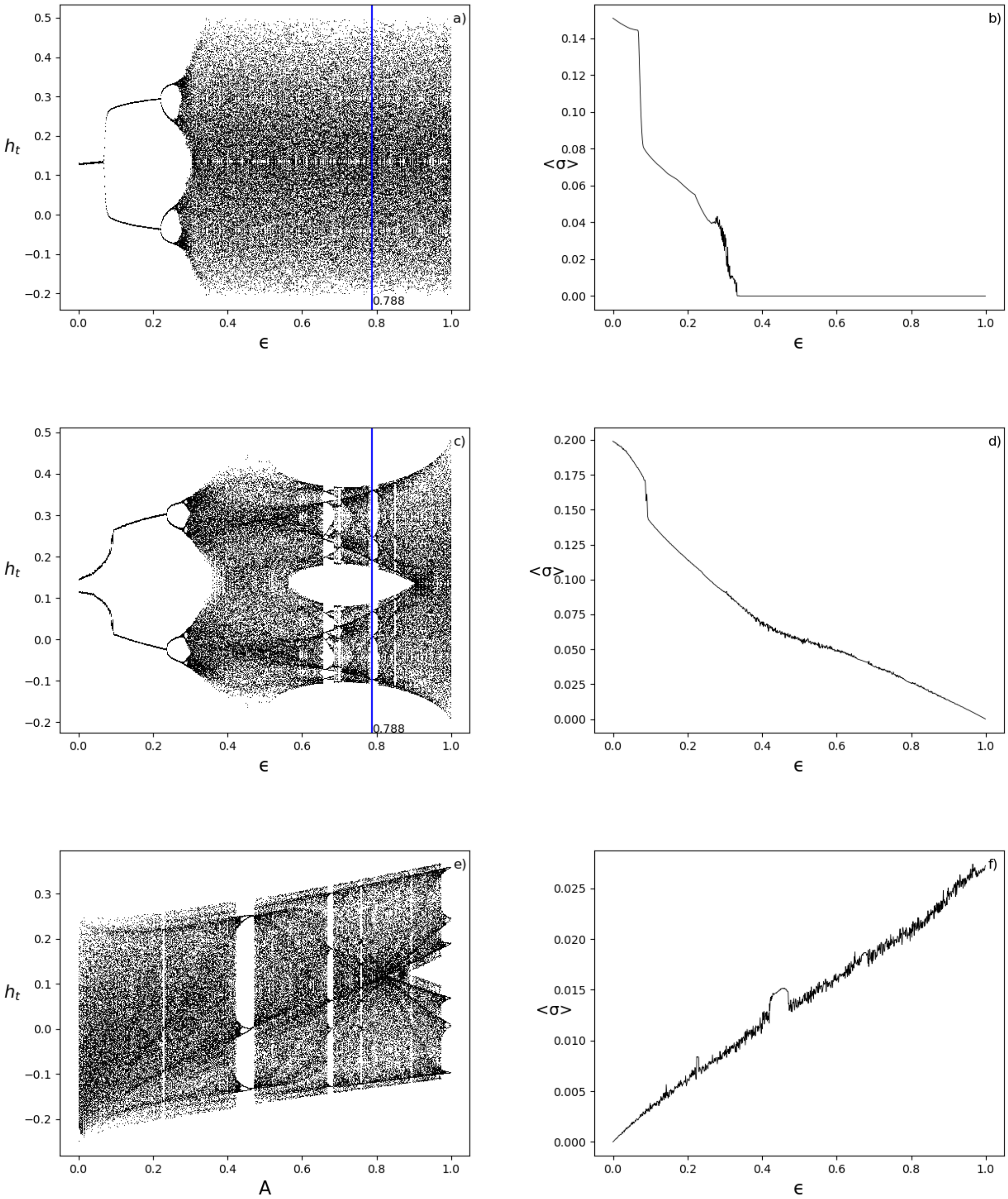

Figure 4.15: Network of globally coupled singular maps Eqs. (4.12) with $z = 0.5$. a)-b) Homogeneous parameters $\mu_i = 0.5, \forall i$; bifurcation diagram for the mean field h_t vs. ϵ and $\langle\sigma\rangle$ vs. ϵ. c)-d) Maximum heterogeneity $\mu_i \in [0.25, 0.75]$; bifurcation diagram for the mean field h_t vs. ϵ and $\langle\sigma\rangle$ vs. ϵ. The blue line signals the value $\epsilon = 0.788$. e)-f) Fixed coupling $\epsilon = 0.788$; bifurcation diagram for the mean field h_t vs. A and $\langle\sigma\rangle$ vs. A. In all graphs, initial conditions are uniformly distributed on the interval $x_0^i = [-8, 2]$, system size $N = 10^5$. For each value of ϵ and A, 10^2 iterates are shown, after discarding 10^3 transients.

4.2.3 Heterogeneous network of pincers maps: bounded robust chaos

In this section we explore the globally coupled network, Eqs. (4.1), for the local dynamics known as pincers map[45], which has been proposed for a model of neuronal network with robust chaos dynamics. It is given by the function

$$x_{t+1} = f(x_t) = \left|\tanh(s(x_t - c))\right|. \tag{4.16}$$

For some ranges of the parameters c and s, the map Eq. (4.16) possesses robust chaos. In particular, for the value $s = 1.3$, there is a robust chaos interval for $c \in [0.1, 0.38]$ according to Ref.[45]. The pincers map is singular at $x = c$, but its iterates are bounded, so that it may represent realistic systems. The corresponding bifurcation diagram as a function of c is displayed in Fig. (4.16)a and the time series of the map for a value of c in the robust chaos interval is shown in Fig. (4.16)b.

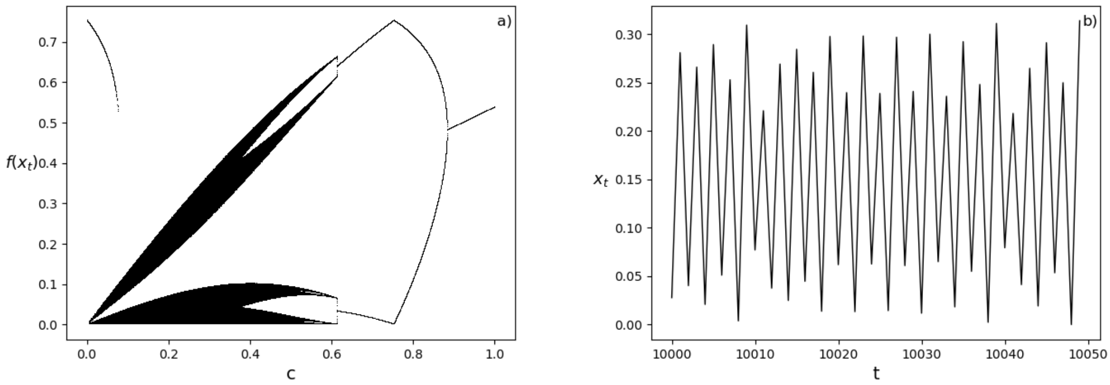

Figure 4.16: a) Bifurcation diagram for the pincer map Eq. (4.16) as a function of c, with fixed value $s = 1.3$, calculated over 200 iterations for each value of c, after discarding 10^4 iterations. b) Time series for $s = 1.3$, $c = 0.25$.

Homogeneous parameters

The network of homogeneous coupled pincers maps is constructed by using Eqs. (4.1) with the local dynamics Eq. (4.16) with uniform parameters s and c. We use the fixed parameter $s = 1.3$ and $c_i = 0.1$, $\forall i$. Figure (4.17) shows the bifurcation diagram of the mean field h_t and the mean standard deviation $\langle\sigma\rangle$ as a function of the coupling ϵ.

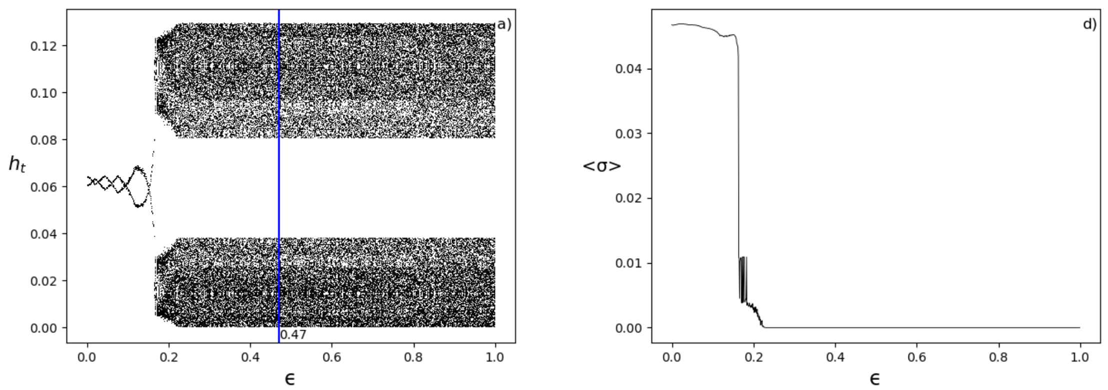

Figure 4.17: Globally coupled homogeneous pincers maps with $s = 1.3, c_i = 0.1$. a) h_t vs. ϵ. For each value of ϵ, 10^2 iterates are shown after 10^3 transients. b) $\langle\sigma\rangle$ vs. ϵ. Initial conditions are uniformly distributed $x_0^i \in [-0.3, 0.78]$, $N = 10^5$.

Asymmetry induced nontrivial collective behavior

Consider the network of globally coupled pincers maps Eqs. (4.1) with local dynamics Eq. (4.16) having fixed value $s = 1.3$ and parameters c_i distributed in a robust chaos range $c_i \in [0.1, 0.38]$ according to Eq. (4.2) as

$$c_i = 0.1 + A\,\xi\,(0.38 - 0.1). \tag{4.17}$$

Figure (4.18)a shows the bifurcation diagram of the mean field h_t as a function of the asymmetry parameter A. For $A = 0$, the system is homogeneous with parameters $c_i = 0.1$, $\forall i$, and h_t displays two chaotic bands. As A increases, periodic windows appear in h_t. For $A \to 1$, the system is fully heterogeneous and h_t exhibits a period-four orbit, while the system is desynchronized.

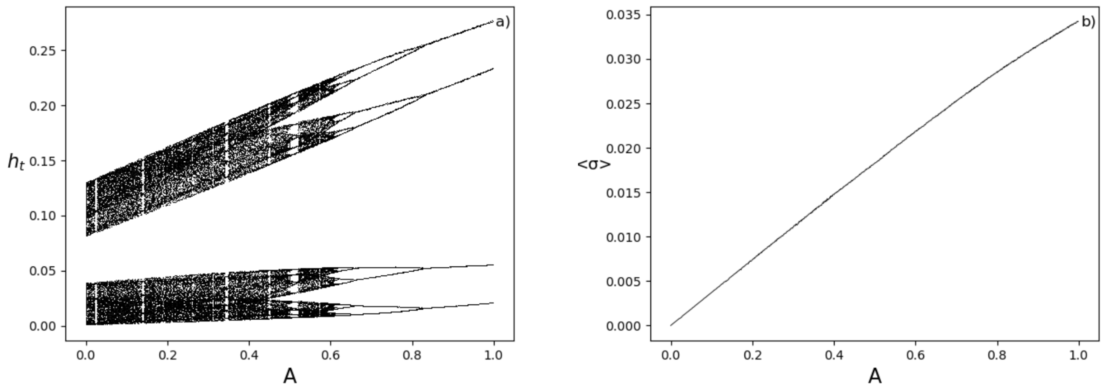

Figure 4.18: Globally coupled heterogeneous pincers maps with $s = 1.3, \epsilon = 0.47$ (blue line in Fig, (4.17)a), and asymmetry parameter A according to Eq. (4.17). a) Bifurcation diagram of h_t vs. A, . b) $\langle\sigma\rangle$ vs. A. Initial conditions are $x_0^i \in [-0.3, 0.78]$. Both graphs were calculated over 10^2 iterations after discarding 10^3 transients. Size $N = 10^5$.

Maximum heterogeneity

Figure (4.19) shows the bifurcation diagram of the mean field h_t and the mean standard deviation $\langle\sigma\rangle$ as functions of the coupling ϵ for the fully heterogeneous system with $A = 1$, $c_i \in [0.1, 0.38]$. A beautiful period-doubling sequence emerges in the collective behavior of system Fig. (4.19)a.

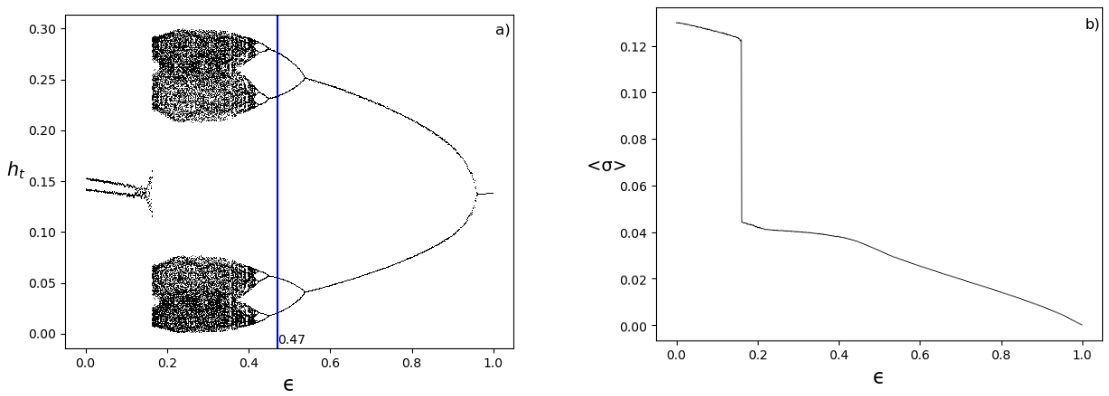

Figure 4.19: Heterogeneous network of pincers maps with $A = 1$, size $N = 10^5$. a) h_t vs. ϵ. b) $\langle\sigma\rangle$ vs ϵ. Initial conditions $x_0^i \in [-0.3, 0.78]$. Both graphs were calculated over 10^2 iterations after neglecting 10^3 iterates.

Other parameters for the pincers map

The robust chaos region and the fixed points on the parameter c of the pincers map Eq. (4.16) depend on the value of s. Figure (4.20) shows the pincer map function $f(x)$.

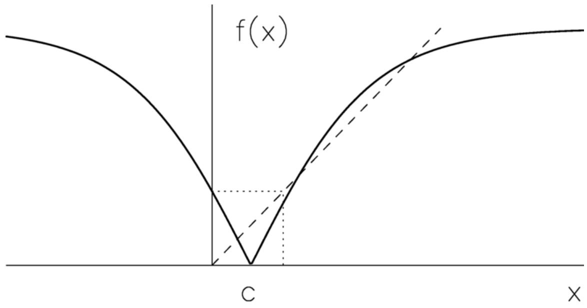

Figure 4.20: Pincers map function $f(x) = \left|\tanh(s(x-c))\right|$ as a function of x. The map is singular at the value $x = c$.

Figure (4.21) shows the bifurcation diagram of the pincer map as a function of c for fixed value $s = 1.7$. Robust chaos occurs in the interval $c \in [0.25, 0.43]$ according to Ref.[45], which we can see in Fig. (4.21)a. The chaotic time series of the map for the parameter $c = 0.25$ is shown in Fig.(4.21)b.

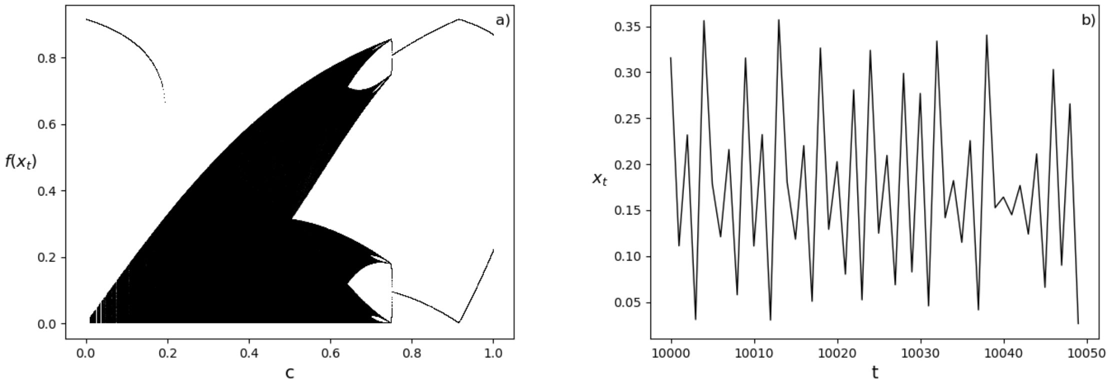

Figure 4.21: a) Bifurcation diagram for the pincers map Eq. (4.16) with fixed parameter $s = 1.7$ as a function of c Robust chaos occurs in the interval $c \in [0.25, 0.43]$. For each value of c, 200 iterates are plotted, after discarding 10^3 transient iterations. b) Time series of the pincers map Eq. (4.16) with fixed $s = 1.7, c = 0.25$. 50 iterations are plotted after discarding 10^4 transients.

In Figure (4.22) we show bifurcation diagrams of the mean field h_t and the mean standard deviation $\langle\sigma\rangle$ for the homogeneous, fully heterogeneous, and asymmetry-dependent globally coupled network Eqs. (4.1) with pincers maps given by Eq. (4.16) with fixed local parameter $s = 1.7$ and varying c.

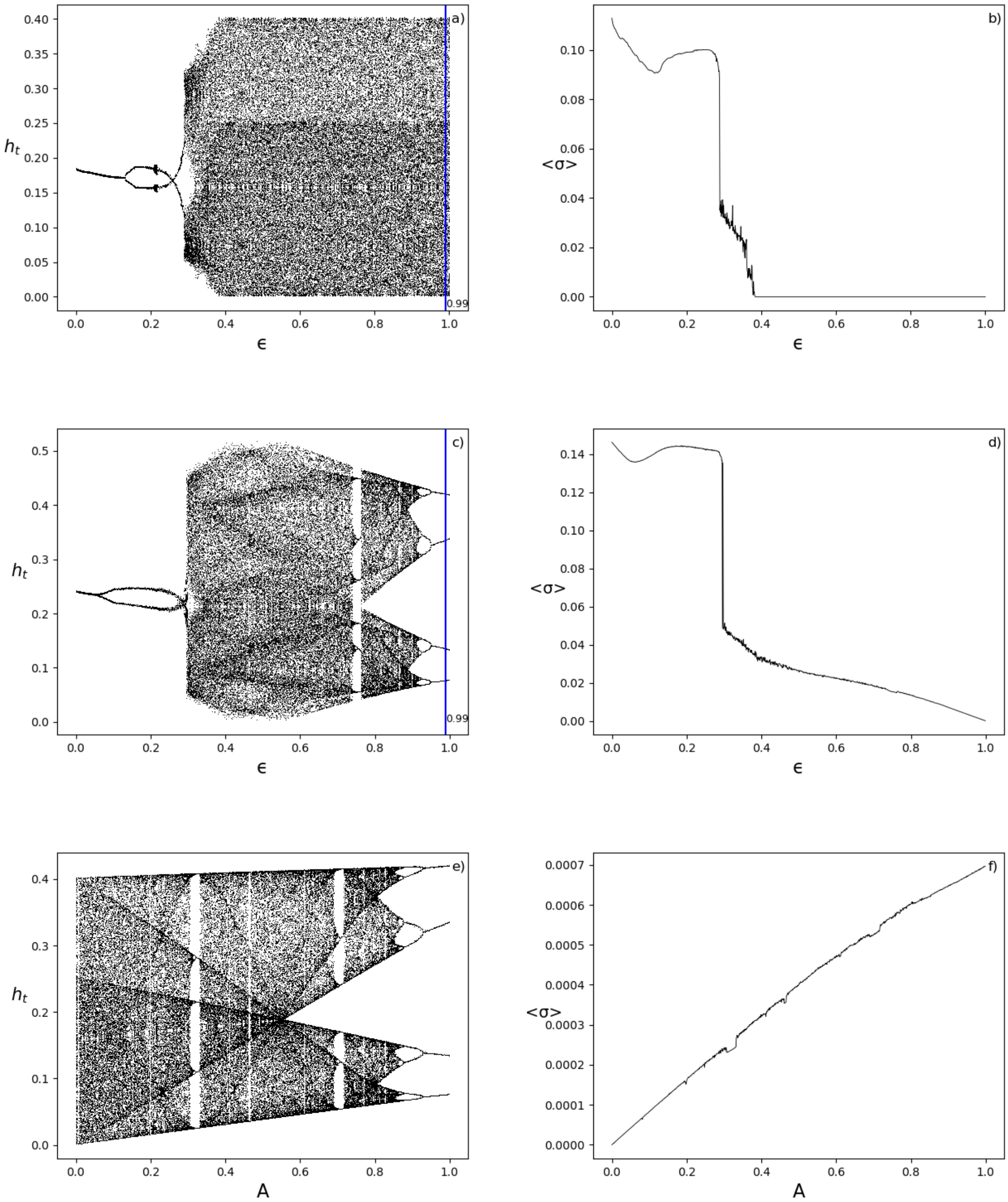

Figure 4.22: Network of globally coupled maps Eqs. (4.1) with pincers maps given by Eq. (4.16) with fixed local parameter $s = 1.7$. a)-b) Homogeneous parameters $c_i = 0.25$, $\forall i$; bifurcation diagram for the mean field h_t vs. ϵ and $\langle \sigma \rangle$ vs. ϵ. c)-d) Maximum heterogeneity $c_i \in [0.25, 0.43]$; bifurcation diagram for the mean field h_t vs. ϵ and $\langle \sigma \rangle$ vs. ϵ. The blue line signals the value $\epsilon = 0.99$. e)-f) Fixed coupling $\epsilon = 0.99$; bifurcation diagram for the mean field h_t and $\langle \sigma \rangle$ vs. the asymmetry parameter A. In all graphs, initial conditions are uniformly distributed on the interval $x_0^i = [-0.19, 0.87]$, system size $N = 10^5$. For each value of ϵ and A, 10^2 iterates are shown, after discarding 10^3 transients.

Period-five collective dynamics induced by asymmetry

In Fig (4.23)a we report an odd-period collective behavior observed in the bifurcation diagram of the mean field h_t of the pincers map network induced by asymmetry. A zoom-in version is shown in Fig (4.23)b. This five-period orbit is seen in the time series of h_t (bottom). As we have mentioned, odd periods in the collective dynamics of coupled map networks have not been reported previously to this work.

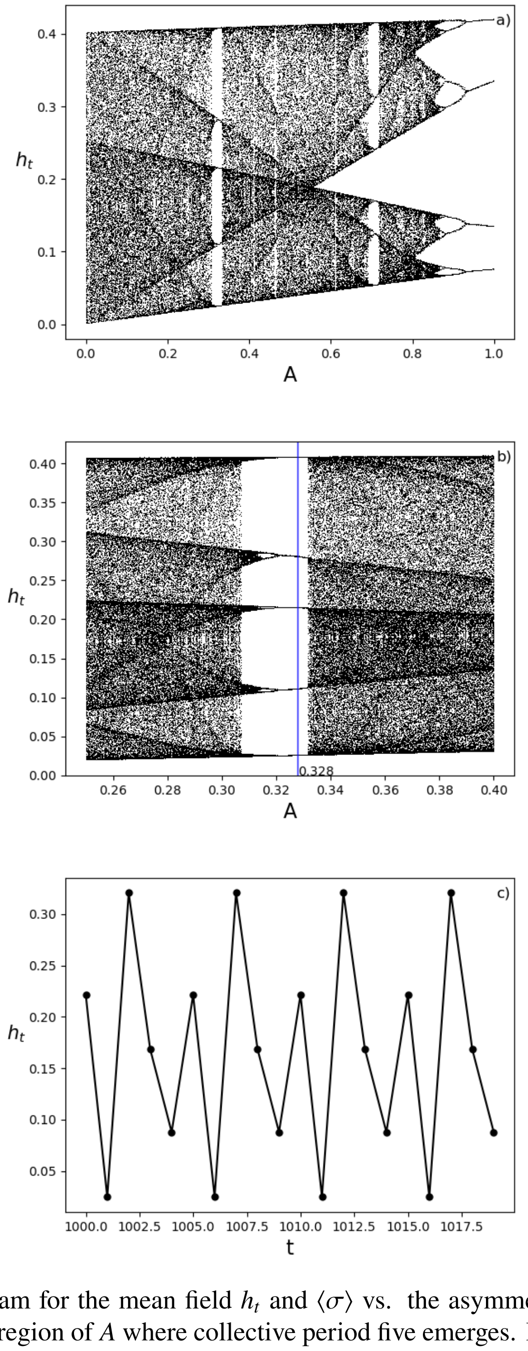

Figure 4.23: a) Bifurcation diagram for the mean field h_t and $\langle\sigma\rangle$ vs. the asymmetry parameter A with fixed coupling $\epsilon = 0.99$. b) Magnification of the region of A where collective period five emerges. Blue line signals the value $A = 0.328$. c) Time series of the mean field h_t for the asymmetry value $A = 0.328$.

4.2.4 Heterogeneous network of smooth maps with robust chaos

So far, we have studied the collective behavior of heterogeneous networks when the local robust chaos maps are discontinuous or have a discontinuous derivative. Here we consider a local map given by[46]

$$f(x_t) = \sin^2\left[r \arcsin(\sqrt{x_t})\right]. \tag{4.18}$$

This map is bounded in the interval $x_t \in [0, 1]$ and possesses robust chaos for $r > 1$, as the bifurcation diagram of Figure (4.24)a shows. The chaotic time series of the map for $r = 2$ is plotted in Fig. (4.24)b.

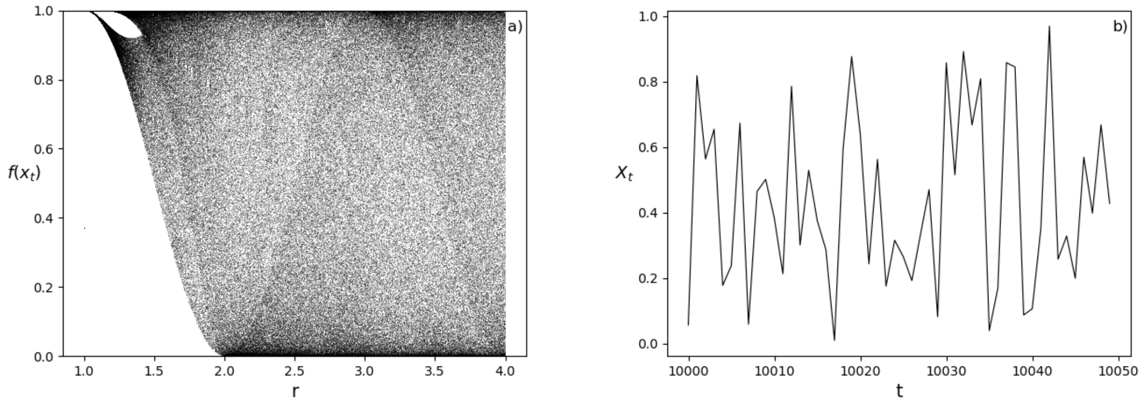

Figure 4.24: a) Bifurcation diagram of the map Eq. (4.18) as a function of r. b) Time series dynamics for $r = 2$ over 50 iterations. Both graphs were obtained after discarding 10^4 transients.

Homogeneous parameters

We consider a globally coupled map network Eqs. (4.1) with the local maps Eq. (4.18) having homogeneous parameters $r_i = 3$, $\forall i$. Figure (4.25) shows the bifurcation diagram of the mean field h_t and the mean standard deviation $\langle\sigma\rangle$ as a functions of the coupling ϵ.

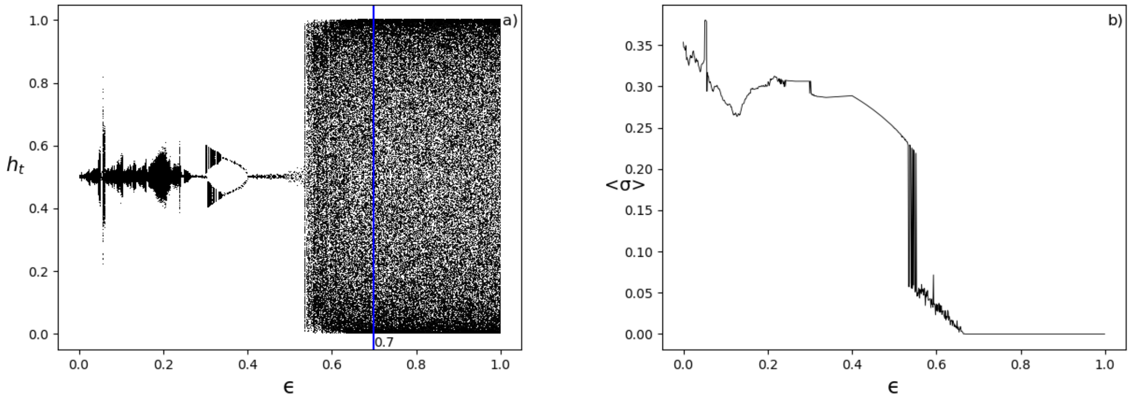

Figure 4.25: a) Bifurcation diagram for the mean field h_t vs ϵ for the homogeneous coupled map network, Eqs. (4.1), with local maps Eq. (4.18) and $r_i = 3, \forall i$. The blue vertical line signals the onset of synchronization. b) Mean standard deviation $\langle\sigma\rangle$ vs. ϵ. Initial conditions are in the interval $x_0^i = [0, 1]$. For each value of ϵ, 200 iterations are taken after discarding 10^3 transients. System size $N = 10^5$.

Different types of synchronization states, including dynamical clusters and chimeras, have been found in the spatiotemporal patterns of this homogeneous system[6]. In particular, for $r = 3$ and $\epsilon = 0.235$ a chimera state with two clusters and a coexisting chaotic subset has been observed[6].

Asymmetry-induced non-trivial collective behaviour

We consider the globally coupled map network Eqs. (4.1) with the smooth local maps Eq. (4.18) having parameters $r_i \in [1.1, 4]$ distributed in the robust chaos range according to Eq. (4.2) as

$$r_i = 1.1 + A\,\xi\,(4 - 1.1). \tag{4.19}$$

Figure (4.26) shows the bifurcation diagram of the mean field h_t and the mean standard deviation $\langle\sigma\rangle$ as a functions of the asymmetry parameter A for the fixed value of coupling $\epsilon = 0.7$.

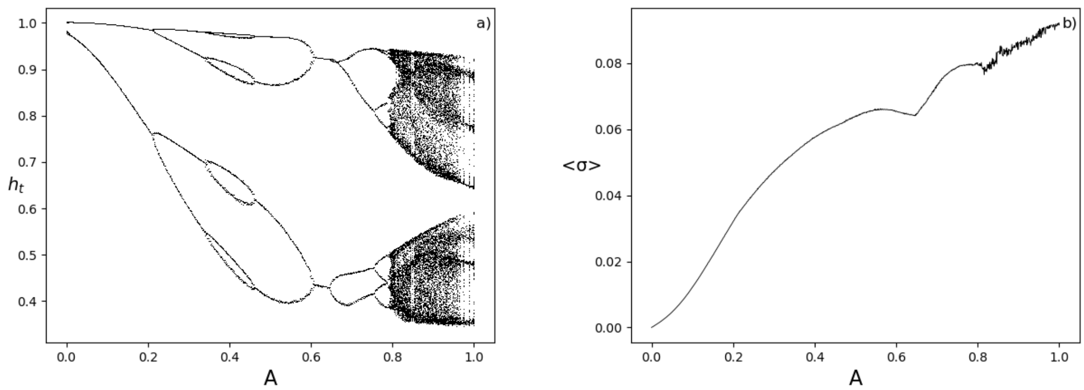

Figure 4.26: Globally coupled Smooth maps with $\epsilon = 0.7$: a) Bifurcation diagram for the mean field of the network h_t vs A heterogeneity parameter. Initial condition in $x_0^i \in [0, 1]$ and all local parameter values varies from Symmetry state parameters $\mu = 1.1$ to heterogeneous state parameters in $\mu \in [1.1, 4]$. b) Time average standard deviation $<\sigma>$ vs A heterogeneity parameter. Both graphs were calculated over 10^2 iterations after neglecting 10^3 iterates in a system size $N = 10^5$ nodes.

Figure (4.26)a shows the rich dynamical collective behavior induced by the asymmetry: period-doubling and bubble bifurcations emerge which are not present in the collective behavior of the homogeneous system. Such nontrivial collective behavior cannot be inferred from the dynamics of an individual smooth map seen in Figure (4.24).

Chapter 5

Conclusions

In this Thesis we have studied the effects that heterogeneity has on the emergence of collective behavior in dynamical networks, other than the synchronization induced by asymmetry discovered by Nishikawa and Motter[5] in 2016.
As dynamical networks, we have investigated coupled map systems globally coupled through their mean field. We have employed two classes of maps possessing robust chaos on a finite interval of their parameters as local dynamical units of the network, unbounded maps (logarithmic, singular) and bounded maps (pincers, smooth). In particular the pincers map has served as model to study neural dynamics[45]. The existence of robust chaos in the constitutive elements means that the emergence of ordered collective behavior in the system cannot be attributed to the presence of stable windows of periodicity in the local dynamics. Thus, any emergent collective behavior must be the product of interactions, which is a characteristic property of complex systems. In addition, the use of maps with bounded robust chaos dynamics represent more realistic systems in contrast to unbounded maps.
An important contribution of this thesis has been to characterize diversity by using an asymmetry control parameter that measures the degree of heterogeneity on a scale from zero (homogeneity) to one (maximum heterogeneity). It should be noted that Nishikawa and Motter[5], in their papers about the phenomenon of asymmetry-induced symmetry with coupled oscillators, do not characterize heterogeneity as a function of an equivalent parameter. The asymmetry parameter A can be treated as a continuous bifurcation parameter for the mean field of the system, providing a way to study the emergence of collective behavior from a homogeneous to a fully heterogeneous complex network. We emphasize that the asymmetry parameter A characterizes the size of the domain where local robust chaos parameters are randomly distributed, so the observed nontrivial collective behavior cannot be attributed to periodic windows that may occur in any of the elements, leaving heterogeneity or asymmetry in the parameters as the direct cause of this phenomenon.
Another relevant finding of this thesis has been the observation of several odd periods (period three, period five) in the nontrivial collective behavior as indicated by the mean field. Period three orbits are typical of unimodal maps[47]. To our knowledge, such behaviors have not been observed before*
In the case of logarithmic and singular maps, heterogeneity in the local parameters does not destroy the periodic collective behavior present in the homogeneous system. The mean field h_t displays orbits of periods 2, 4, 8, 16, as a function of the coupling parameter, similar to the period-doubling bifurcation characteristic of smooth unimodal maps possessing a single maximum or minimum. However, these maps do not possess any periodic orbits on the interval considered, and they do not belong to the universal class of smooth unimodal maps. Thus, the mean field h_t has acquired properties that are not present in the local maps. Therefore, the period-doubling behavior observed in the mean field is a emergent nontrivial collective property of these systems. Furthermore, heterogeneity can induce complex collective behavior, such as the bubble bifurcations in the mean field of the smooth robust chaos map.

*H. Chaté, private communication to M. Cosenza.

In summary, our results reveal that heterogeneity in the parameters of the local elements of a dynamical network can induce a variety of ordered, periodic nontrivial collective behavior, other than synchronization, in situations where such behavior does not exist if the system is homogeneous. Our research is relevant in many systems where heterogeneity and diversity of the elements are inherent or very common, such as social and biological systems.

Bibliography

[1] Boccara, N.; Boccara, N. *Modeling complex systems*; Springer, 2010; Vol. 1.

[2] Kaneko, K.; Tsuda, I. *Complex Systems: Chaos and Beyond: A Constructive Approach With Applications in Life Sciences*; Springer Science & Business Media, 2001.

[3] Newman, M. E. Networks: An Introduction. (Oxford University Press),, 772 pages. ISBN-978-0-19-920665-0. 2012.

[4] Pikovsky, A.; Rosenblum, M.; Kurths, J.; Synchronization, A. A universal concept in nonlinear sciences. *Self* **2001**, *2*, 3.

[5] Nishikawa, T.; Motter, A. E. Symmetric states requiring system asymmetry. *Physical Review Letters* **2016**, *117*, 114101.

[6] Cosenza, M. G.; Alvarez-Llamoza, O.; Cano, A. V. Chimeras and clusters emerging from robust-chaos dynamics. *Complexity* **2021**, *2021*, 8878301.

[7] Chate, H.; Manneville, P. Collective behaviors in coupled map lattices with local and nonlocal connections. *Chaos: An Interdisciplinary Journal of Nonlinear Science* **1992**, *2*, 307–313.

[8] Manrubia, S. C.; Mikhailov, A. S.; Zanette, D. *Emergence of dynamical order: synchronization phenomena in complex systems*; World Scientific, 2004; Vol. 2.

[9] Molnar, F.; Nishikawa, T.; Motter, A. E. Network experiment demonstrates converse symmetry breaking. *Nature Physics* **2020**, *16*, 351–356.

[10] Sugitani, Y.; Zhang, Y.; Motter, A. E. Synchronizing chaos with imperfections. *Physical Review Letters* **2021**, *126*, 164101.

[11] Zhang, Y.; Motter, A. E. Mechanism for strong chimeras. *Physical Review Letters* **2021**, *126*, 094101.

[12] Molnar, F.; Nishikawa, T.; Motter, A. E. Asymmetry underlies stability in power grids. *Nature communications* **2021**, *12*, 1457.

[13] Palacios, A. Synchronization in asymmetrically coupled networks with homogeneous oscillators. *Physical Review E* **2021**, *103*, 022206.

[14] Gu, C.; Wang, P.; Weng, T.; Yang, H.; Rohling, J. Heterogeneity of neuronal properties determines the collective behavior of the neurons in the suprachiasmatic nucleus. *Mathematical Biosciences and Engineering* **2019**, *16*, 1893–1913.

[15] Kaneko, K. Globally coupled chaos violates the law of large numbers but not the central-limit theorem. *Physical Review Letters* **1990**, *65*, 1391.

[16] Cosenza, M. G.; González, J. Synchronization and collective behavior in globally coupled logarithmc maps. *Progress of Theoretical Physics* **1998**, *100*, 21–38.

[17] Cisneros, L.; Jiménez, J.; Cosenza, M. G.; Parravano, A. Information transfer and nontrivial collective behavior in chaotic coupled map networks. *Physical Review E* **2002**, *65*, 045204(R).

[18] Kaneko, K. Theory and Applications of Coupled Map Lattices. *Chaos, Focus issue in Coupled Map Lattices* **1992**, *2*.

[19] Kaneko, K. Period-doubling of kink-antikink patterns, quasiperiodicity in antiferro-like structures and spatial intermittency in coupled logistic lattice: Towards a prelude of a "field theory of chaos". *Progress of Theoretical Physics* **1984**, *72*, 480–486.

[20] Waller, I.; Kapral, R. Spatial and temporal structure in systems of coupled nonlinear oscillators. *Physical Review A* **1984**, *30*, 2047.

[21] Cosenza, M. G.; Kapral, R. Coupled maps on fractal lattices. *Physical Review A* **1992**, *46*, 1850.

[22] Kaneko, K. From globally coupled maps to complex-systems biology. *Chaos: An Interdisciplinary Journal of Nonlinear Science* **2015**, *25*, 097608.

[23] Cosenza, M. G.; Parravano, A. Dynamics of coupling functions in globally coupled maps: Size, periodicity, and stability of clusters. *Physical Review E* **2001**, *64*, 036224.

[24] Pikovsky, A.; Rosenblum, M. Dynamics of globally coupled oscillators: Progress and perspectives. *Chaos: An Interdisciplinary Journal of Nonlinear Science* **2015**, *25*, 097616.

[25] Schimansky-Geier, L. Kuramoto, Y., Chemical Oscillations, Waves, and Turbulence. Berlin-Heidelberg-New York-Tokyo, Springer-Verlag 1984. VIII, 156 S., 41 Abb., DM 79,—. US. 1986.

[26] Nakagawa, N.; Kuramoto, Y. From collective oscillations to collective chaos in a globally coupled oscillator system. *Physica D: Nonlinear Phenomena* **1994**, *75*, 74–80.

[27] Grüner, G. The dynamics of charge-density waves. *Reviews of Modern Physics* **1988**, *60*, 1129.

[28] Wiesenfeld, K.; Hadley, P. Attractor crowding in oscillator arrays. *Physical Review Letters* **1989**, *62*, 1335.

[29] Wiesenfeld, K.; Bracikowski, C.; James, G.; Roy, R. Observation of antiphase states in a multimode laser. *Physical review letters* **1990**, *65*, 1749.

[30] Newman, M. E.; Barabási, A.-L. E.; Watts, D. J. *The structure and dynamics of networks.*; Princeton University Press, 2006.

[31] Meyers, R. A. *Encyclopedia of complexity and systems science*; Springer New York, 2009; Vol. 9.

[32] González-Avella, J. C.; Cosenza, M. G.; Tucci, K. Nonequilibrium transition induced by mass media in a model for social influence. *Physical Review E* **2005**, *72*, 065102.

[33] González-Avella, J. C.; Cosenza, M. G.; Eguíluz, V. M.; San Miguel, M. Spontaneous ordering against an external field in non-equilibrium systems. *New Journal of Physics* **2010**, *12*, 013010.

[34] González-Avella, J. C.; Cosenza, M. G.; San Miguel, M. Localized coherence in two interacting populations of social agents. *Physica A: Statistical Mechanics and its Applications* **2014**, *399*, 24–30.

[35] Cosenza, M. G.; Gavidia, M.; González-Avella, J. C. Against mass media trends: Minority growth in cultural globalization. *Plos One* **2020**, *15*, e0230923.

[36] Garcia-Ojalvo, J.; Elowitz, M. B.; Strogatz, S. H. Modeling a synthetic multicellular clock: repressilators coupled by quorum sensing. *Proceedings of the National Academy of Sciences* **2004**, *101*, 10955–10960.

[37] Wang, W.; Kiss, I. Z.; Hudson, J. Experiments on arrays of globally coupled chaotic electrochemical oscillators: Synchronization and clustering. *Chaos: An Interdisciplinary Journal of Nonlinear Science* **2000**, *10*, 248–256.

[38] De Monte, S.; d'Ovidio, F.; Danø, S.; Sørensen, P. G. Dynamical quorum sensing: Population density encoded in cellular dynamics. *Proceedings of the National Academy of Sciences* **2007**, *104*, 18377–18381.

[39] Taylor, A. F.; Tinsley, M. R.; Wang, F.; Huang, Z.; Showalter, K. Dynamical quorum sensing and synchronization in large populations of chemical oscillators. *Science* **2009**, *323*, 614–617.

[40] Tinsley, M. R.; Nkomo, S.; Showalter, K. Chimera and phase-cluster states in populations of coupled chemical oscillators. *Nature Physics* **2012**, *8*, 662–665.

[41] Hagerstrom, A. M.; Murphy, T. E.; Roy, R.; Hövel, P.; Omelchenko, I.; Schöll, E. Experimental observation of chimeras in coupled-map lattices. *Nature Physics* **2012**, *8*, 658–661.

[42] Kaneko, K. Clustering, coding, switching, hierarchical ordering, and control in a network of chaotic elements. *Physica D: Nonlinear Phenomena* **1990**, *41*, 137–172.

[43] Alvarez-Llamoza, O.; Cosenza, M. G.; Ponce, G. A. Critical behavior of the Lyapunov exponent in type-III intermittency. *Chaos, Solitons & Fractals* **2008**, *36*, 150–156.

[44] Schuster, H.; Just, W. Deterministic Chaos WILEY. 2005.

[45] Potapov, A.; Ali, M. Robust Chaos in neural networks. *Physics Letters A* **2000**, *277*, 310–322.

[46] Aguirregabiria, J. M. Robust chaos with prescribed natural invariant measure and Lyapunov exponent. *arXiv preprint arXiv:0907.3790* **2009**,

[47] Li, T.-Y.; Yorke, J. A. Period three implies chaos. *The American Mathematical Monthly* **2004**, *82*, 985–992.

Appendices

Appendix A

Python code for Asymmetry parameter

The following code is made in python. The globally coupled map network Eqs.(4.1) with The local dynamics considered for Eq.(4.18):

```
"""@author: KARG"""
import matplotlib.pyplot as plt
import numpy as np
import time

#--------------------------timer start---------------------------------
start=time.time()

#--------------------------Functions-----------------------------------
def f(x,r):
    return np.sin(r*(np.arcsin(np.sqrt(x))))**2  #Local map
def Xn(fxn):
    mean_fxn = fxn.mean()
    return (1-e)*fxn + (e*mean_fxn)              #Globally coupled maps

#---------------------------Initial conditions-------------------------
N=10000                     #System size
it=200                      #iterations
drop=1000                   #dropped terms
e=.7                        #coupling parameter
R1,R2=1.1,4                 #Robust Chaos interval
a=np.linspace(0,1,1000)     #Asymmetry parameter A
xpoints=[]
hpoints=[]
V=[]

#-------------------------Initialization--------------------------------
for A in a :
    vpoints=[]
```

```
    xold=np.random.uniform(0,1,N)
    R=np.random.uniform(0,1,N)
    ri=R1+A*R*(R2-R1)
    for t in range (0,drop+it):
        if t>=drop:
            xpoints.append(A)
            hpoints.append(np.mean(xold))      #h_t
            vpoints.append(np.std(xold))
        fxn=f(xold,ri)
        xold=Xn(fxn)
    V.append(np.mean(vpoints))                 #<sigma>

#--------------------------NTCB Plots-----------------------------------
plt.plot(xpoints,hpoints, ',k',linewidth=.61, alpha=.90)
plt.xlabel('$A$',fontsize=16)
plt.ylabel(r'$h_{t}$',labelpad=10,rotation=0,fontsize=15)
#plt.savefig('Asymmetry_Unimodal.eps', format='eps')

#----------------------Synchronization Plots----------------------------
"""
plt.plot(A,V,ls='-',color='k',linewidth=.61, alpha=1)
plt.xlabel('A',fontsize=16)
plt.ylabel('<\sigma>',labelpad=10,rotation=0,fontsize=14)
plt.savefig('STD_Asymmetry_Unimodal.eps', format='eps')
"""

#---------------------------timer end------------------------------------
end=time.time()
codetime=(end-start)/60     #expressed in min
print("code t ime",round(codetime,2),"min")
```